Université d'Ottawa · University of Ottawa

Université d'Ottawa · University of Ottawa

FACULTÉ DES ÉTUDES SUPÉRIEURES ET POSTDOCTORALES

FACULTY OF GRADUATE AND POSTDOCTORAL STUDIES

Peter MACSWEEN

AUTEUR DE LA THÈSE - AUTHOR OF THESIS

M. A. Sc. (Electrical Engineering)

GRADE - DEGREE

School of Information Technology and Engineering

FACULTÉ, ÉCOLE, DÉPARTEMENT - FACULTY, SCHOOL, DEPARTMENT

TITRE DE LA THÈSE - TITLE OF THE THESIS

Resource Allocation for Radar Signal Interception in ESM Receivers

É. Dubois

DIRECTEUR DE LA THÈSE - THESIS SUPERVISOR

J-F. Rivest

CO-DIRECTEUR DE LA THÈSE - THESIS CO-SUPERVISOR

EXAMINATEURS DE LA THÈSE - THESIS EXAMINERS

M. Bouchard

R. Dansereau

J.-M. De Koninck, Ph.D.

LE DOYEN DE LA FACULTÉ DES ÉTUDES SUPÉRIEURES ET POSTDOCTORALES

DEAN OF THE FACULTY OF GRADUATE AND POSTDOCTORAL STUDIES

Resource Allocation for Radar Signal Interception in ESM Receivers

Peter J.A.F. MacSween

Ottawa-Carleton Institute for Electrical & Computer Engineering
School of Information Technology & Engineering (SITE)
University of Ottawa
Ottawa, Canada

November 2004

A thesis submitted to the School of Graduate Studies and Research in partial fulfillment of the requirements of the degree of Master of Applied Science.

2004/11/10

Your file Votre référence
ISBN: 0-494-01541-1
Our file Notre référence
ISBN: 0-494-01541-1

Abstract

Electronic Support Measures (ESM) receivers exist that are capable of detecting the transmissions from radar emitters in a robust and reliable manner. Typically, the receiver operator wishes to detect the transmitted signals from a known set of emitters as quickly as possible. To achieve this, a schedule is created that dictates the order in which the receiver will search for the various emitters. Techniques exist for predicting the maximum time to intercept between a receiver and an emitter, but they only work from known scheduling parameters. The quantity of emitters and the density of their signals typically prevents a naive approach to generating the schedule.

The purpose of this thesis was to generate scanning receiver schedules that minimize the maximum time to intercept for a set of scanning emitters. Genetic algorithms and the use of pulse train theory were combined to generate the schedules in an automated fashion.

The genetic algorithm consistently produced ESM receiver schedules that used duration values for each frequency band that were near the largest scan rate of all the emitters in each band. This was an unexpected result and demonstrated that the minimization of the maximum intercept time for a set of emitters can be accomplished using the maximum scan values.

A new scheduling algorithm was created that utilized the maximum scan values. It generated ESM receiver schedules that were equivalent to the best schedules produced by the genetic algorithm scheduler, and produced them with much less computational effort.

Acknowledgments

This work would not have been possible without the support of many others. Firstly, I would like to express my appreciation for the encouragement and direction provided by my thesis advisor, Dr. Jean-François Rivest. Dr. Pierre Lavoie at Defense Research and Development Canada Ottawa I thank for providing access to office and computing facilities.

Major Linda Hatton and Major Dan Martella of the Canadian Forces I thank for having faith in my potential. Ms. Melanie Yeretch at the Canadian Forces Support Unit (Ottawa) I thank for all the administrative support. Ms. Lucette Lepage at the University of Ottawa I thank for her prompt and efficient administration of the intricacies of my file.

Most importantly, I thank my wife Patty for the care, love, and support she provided which allowed me to see this work through to completion.

Contents

List of Figures

List of Tables

Chapter 1

Introduction

1.1 Motivation

The necessity of the modern military force is founded on a variety of historical, economic, geographical and political imperatives. The success of that modern fighting force has traditionally been dependent on discipline, skill at arms, technology, luck, and the leadership of all the soldiers in positions of authority within the chain of command. The study of past skirmishes, battles and wars has demonstrated that the ability of a commander to 'have a complete picture', or understanding, of the battlefield at the correct level of abstraction has been critical to success.

In modern parlance, this complete picture is referred to as 'battlespace' or 'situational' awareness. One side seeks to gain superiority through the use of increased awareness, while denying, or decreasing the enemy's awareness.

The original 'battlefield picture' was pieced together from reports generated by scouts and messengers on horseback (personnel dedicated to reconnaissance and communication). The enemy was perceived to be seen or heard (troops, tents, fires, decoys, etc.) at a particular location and that information was conveyed through the chain of command to the appropriate level. Signal flares, telescopes, motorized vehicles, radios, telephones, and many other forms of technology have all improved the accuracy and timeliness of these reports, but the fundamental activities and purpose have not changed.

The modern military is equipped with a bewildering array of battlefield electronics, each relying on various active and passive techniques, and is constructed on the basis

of fundamental physical properties, including electromagnetic propagation, optics, and acoustics. The modern military force is augmented with equipment designed to hear and locate an enemy's presence in any of these mediums. When that presence is detected, details of it are generated for use by the chain of command, improving the commanders ability to 'see' the enemy.

With the increased availability, capability, and reliability of modern equipment, the military has come to rely heavily on the ability to electronically 'see and hear' an enemy force, to protect it's own electronic capabilities, and to exploit any enemy's weaknesses.

Radar is a technology that has been implemented in many forms for many military purposes. It is particularly well suited for the provision of information about enemy forces, on both the land and sea, and in the air. It has been prevalent in the success of military operations since it was developed during the Second World War, and modern radar systems continue to be a factor. As ably demonstrated during the 1999 conflict in Kosovo, simple tactics proved very effective at safeguarding the air defense system [1], denying the coalition air forces complete control of the airspace. Every mission that entered the area of operations required the best electronic warfare support possible.

1.2 Problem Statement

The purpose of this thesis is to combine two fields of study in an attempt to generate scanning receiver schedules that minimize the maximum time to intercept for a set of scanning emitters. Modern optimization algorithms and the use of pulse train theory are combined to generate the schedules in an automated fashion.

One facet of electronic warfare is the interception of radar signals. Receivers exist that are capable of detecting the transmissions from electronic emitters in a robust and reliable manner. This equipment is typically operated in a role where the purpose is to record the transmitted signals from a known set of emitters as quickly as possible. To achieve this, a schedule is created that dictates the order in which a receiver will search for the various emitters. Techniques exist for predicting the maximum time to intercept between a receiver and an emitter, but they only work from known scheduling parameters. The quantity of emitters and the density of their signals typically prevents a naive approach to generating the schedule.

1.3 Contributions

This thesis makes the following contributions:

- Investigates the combination of genetic algorithms as an optimization technique with the use of pulse train theory as an objective function for the purpose of creating an electronic support measures receiver schedule that minimizes the maximum time to intercept.
- Proposes the use of a scheduling algorithm that utilizes the maximum emitter scan rates for each frequency band to generate an electronic support measures receiver schedule that minimizes the maximum time to intercept.

Chapter 2

Electronic Support Measures

The interception of RF signals by electronic support measures (ESM) receivers is a military task that has developed as electronics and the tactics of their use have evolved in the past century. As the earliest radios evolved into modern radars and communications equipment, the first direction-finding equipment also evolved into the wealth of ESM receiver types and architectures available today. Though the technology has changed, the overall purpose is still the same. Electronic Support Measures are:

> That division of electronic warfare involving action taken to search for, intercept, identify and locate radiated electromagnetic energy for the purpose of immediate threat recognition. It provides a source of information required for immediate decisions involving electronic countermeasures, electronic counter-countermeasures and other tactical actions such as avoidance, targeting and homing. [2]

"Search, intercept, identify, and locate" are the major ESM activities, and each of them must be effective for any ESM system to be considered successful. Searching for electromagnetic signals requires the examination of all the possible frequencies of transmission. To intercept a signal, a receiver must be tuned to the emitter frequency at the time the transmission is made. To identify and locate the emitter, the intercepted signal information must be analyzed. Each of these topics are significant areas of study on their own, but the interception of signals is the main activity of interest in this work.

While interception techniques can be used against any electromagnetic signal, the issue under consideration is how they can be used effectively against radar signals.

Radio detection and ranging (RADAR) is used for many purposes. It's reliability in augmenting the human sense of sight to allow objects to be detected in darkness and inclement environmental conditions has resulted in its application as the primary sensor on many major weapons systems. It is the threat of these systems that the use of ESM receivers attempts to limit.

The analysis of the radar interception problem requires an understanding of the characteristics of radar emitters and ESM receivers, which is covered in the following sections.

2.1 Radar Emitters

The radar principle, at its essence, is the detection and analysis of reflected electromagnetic energy. A transmitter and an antenna generate a signal that is bounced off an object (target), and a receiver and an antenna are used to capture the reflected signal. Knowing the start time and speed of the transmitted signal allows the calculation of the range of the object. The radar equation summarizes the relationship between the range of a radar and the various attributes of the radar system, target, and environment [3], and it's derivation is useful in describing the radar principle.

The power density P of a signal at a distance R from a radar transmitter is related to the transmitted power P_T by:

$$P = \frac{P_T}{4\pi R^2}$$

The transmitter normally uses a directional antenna with gain G_T resulting in:

$$P = \frac{P_T G_T}{4\pi R^2}$$

The signal is reflected off the target in proportion to it's radar cross-section δ:

$$P = \frac{P_T G_T \delta}{4\pi R^2}$$

The re-radiated signal is diminished by it's distance back to the receiver:

$$P = \frac{P_T G_T \delta}{(4\pi R^2)^2}$$

And the portion of the reflected signal that is received is proportional to the effective capture area A_e of the antenna:

$$P = \frac{P_T G_T \delta A_e}{(4\pi R^2)^2} = \frac{P_T G_T \delta A_e}{(4\pi)^2 R^4}$$

This simple form of the radar equation makes many ideal assumptions (i.e. free space propagation, refraction, absorption, etc.), and is normally manipulated and extended for specific purposes. It is important to note that the gain G_T and effective antenna area A_e are dependent on the frequency of the transmitted signal.

The parameters of the radar equation are available for manipulation during the design of a radar system, but are generally fixed by the time the equipment is put into operation. Antenna shapes may be constrained for vehicle or aircraft mounting, input power is limited by the available power sources, the gain is a function of the sensitivity of the equipment, but the frequency of transmission is one of the parameters that is available for a system operator to maximize the performance of the radar. Typically, only a set or range of frequencies are available for use, and these are defined as emitter modes. Although the low probability of intercept techniques such as spread-spectrum signals, frequency-hopping transmitters, and distributed antennas are available, the majority of radar systems still use the traditional transmission techniques, and are the systems we wish to study. The first requirement necessary for an intercept to occur is that the ESM receiver must be tuned to the frequency of transmission of the radar emitter at the time the transmission occurs.

Radar systems must radiate electromagnetic energy, and in doing so it is impractical for them to continuously transmit in all directions. The use of an antenna provides greater radar range and greatly improves the performance of a radar system. By moving the antenna, the bearing to a target can easily be calculated from the direction the antenna beam was pointing when the signal from the target was received. By changing the elevation of the antenna, the altitude or height of a target can similarly be calculated. By combining these, a three dimensional volume of space can be scanned, and this scan is typically repeated periodically for continued surveillance of an airspace. The vast majority of in-service radar systems scan in this traditional manner. This generates a problem when attempting to intercept a radar signal, because the narrow electromagnetic beam formed by the antenna is not always pointing at the ESM receiver located

at a point within that volume (the receiver is assumed to have an omni-directional antenna). This results in the second requirement necessary for an interception to occur, which is that the radar system must be transmitting in the direction of the ESM receiver.

The calculation of antenna patterns and the study of the propagation effects of the radar signal are not the focus of this work, so the concept of a scan duty cycle is used to specify that portion of time during an emitters scan period when the signal is detectable by the receiver. This value is dependent on the performance of the particular ESM system. While receivers are typically trying to detect the main lobe of an emitter, some are sensitive enough to detect some of side lobes as well. The ability to detect the side lobes means that a greater portion of the emitters scan can be detected, so the scan duty cycle would be increased accordingly.

The electromagnetic signal that is actually transmitted from a radar system can be one of many different type of waveforms. One of the more typical categories of waveforms is the pulsed waveform, where only small bursts of energy are transmitted at intervals much larger than the width of the pulse (and much smaller than the scan rate). By adjusting the shape of the pulse and the time between pulses, radar systems are able to provide better distinction between targets under various conditions and ranges. The detailed attributes of the possible pulse shape and timing techniques are important to the identification of a radar system, and the identification techniques typically require several pulses from the emitter in order to identify it. To this end, the third requirement necessary for interception is that the receiver must receive a minimum number of pulses from the emitter.

The characteristics of the radar signal that are important to interception are

$$
\begin{aligned}
F &= \text{the RF carrier frequency of transmission} \\
T_{scan} &= \text{the scan period} \\
\lambda_{scan} &= \text{the scan duty cycle} \\
PRI &= \text{the pulse repetition interval}
\end{aligned}
$$

These characteristics are shown pictorially in Figure 2.1. It is important to note that the RF carrier frequency is not related to the scan period, and that the individual radar pulses occur within each scan.

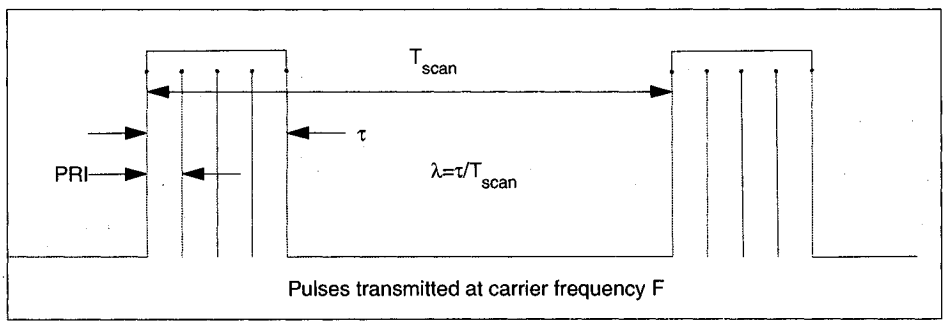

Fig. 2.1 Emitter Characteristics of Importance to Interception

This emitter information is normally available through intelligence means, and is assumed known *a priori* to the calculation of the maximum intercept time.

2.2 ESM Receivers

There are numerous types of ESM receivers and receiver architectures. Each of them has strengths when detecting electromagnetic signals, and each plays a role in the 'search, intercept, identify and locate' aspects of ESM systems. The design of an ESM receiver suffers from two constraints that tend to contradict each other: bandwidth and sensitivity. Wideband receivers can detect emitters across a large bandwidth, but provide poor

sensitivity when capturing the individual signals because the amount of noise entering the system is proportional to the bandwidth. Narrowband receivers provide excellent sensitivity, but only within a narrow bandwidth. Channelized receivers are multiple narrowband receivers operating in parallel, and scanning receivers are narrowband receivers that can re-tune dynamically, moving through various frequency bands (refer to [4] and [5] for further details).

For the purpose of our study of radar interception, we will be concerned with the scanning superheterodyne receiver (SHR). The SHR is commonly used because it can scan a wide bandwidth with good sensitivity and is relatively lightweight. A SHR relies on the principle of heterodyning, or mixing of two signals, which is done to take a high frequency radar signal and create a subsequent signal centered at a lower, intermediate frequency. By adjusting the properties of the mixing signal, various frequency ranges of radar signals can be tuned. The new, lower frequency signal is much easier to filter and analyze since the electronics to do so can be optimized for the intermediate frequency. The SHR is then able to focus on a narrow band of frequencies that are centered at the intermediate frequency. A SHR that implements the electronics to receive and heterodyne multiple bands simultaneously has multiple channels.

In order to scan a range of frequencies larger than that available at the intermediate frequency, the SHR must switch frequency bands by adjusting the mixing signal. The time required to adjust the mixing signal, and for a stable output to appear at the intermediate frequency is referred to as the re-tuning time, t_{tune}. The mixing signal has finite upper and lower limits of $F_{MaxScan}$ and $F_{MinScan}$. The frequency range available at the intermediate frequency dictates the instantaneous bandwidth (BW_{inst}) of the receiver. The number of tuning steps, or frequency bands, required to span the band defined by $F_{MaxScan}$ and $F_{MinScan}$ is simply $(F_{MaxScan} - F_{MinScan} + BW_{inst})/BW_{inst}$. The length of time that the SHR pauses in each frequency band is the duration (d_m where there are M bands). It is during this time that emitters that transmit in frequency band m can be received. A schedule for a SHR then consists of a duration for each frequency band (each of which can be different) which is continuously repeated with period T_{sched}. Figure 2.2 gives a pictorial representation of these parameters.

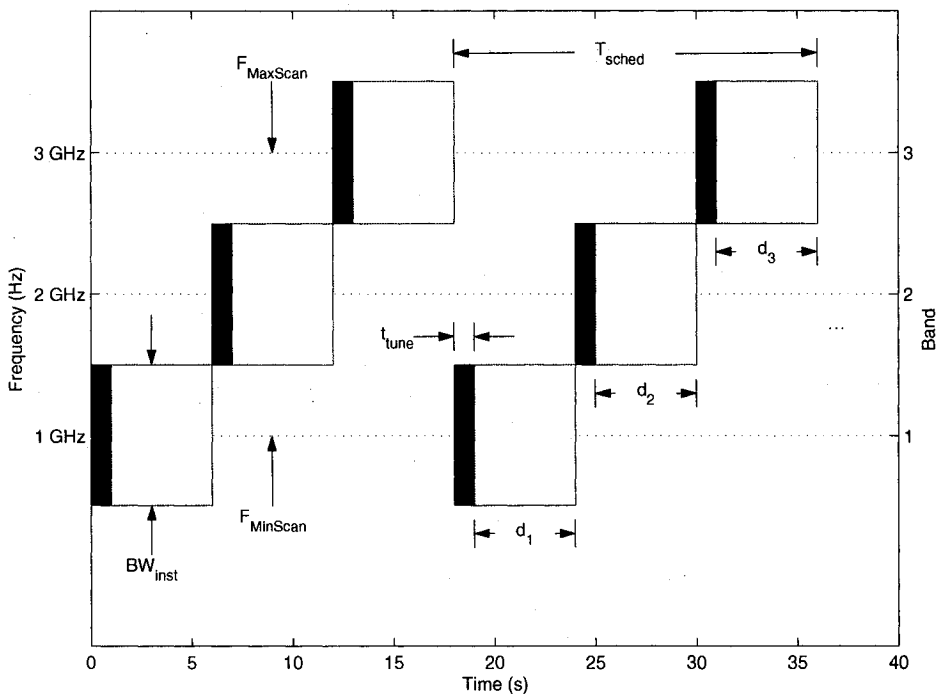

Fig. 2.2 Scanning Superheterodyne Receiver Schedule

2.3 Search and Interception

The density of radar emitters that an ESM receiver wants to intercept is typically very high. The highest density of emitters typically occurs in coastal areas, with the concurrent possibility of sea, land, and airborne emitters. The receiver is limited by the instantaneous bandwidth that it can receive at any particular moment, so it is impossible to intercept all the emitters simultaneously. We want to scan all the frequency bands and ensure that we intercept as many emitters as possible. Considering that the emitters are typically part of a larger weapons system, it is important that they be intercepted within a finite amount of time; we also want this amount of time to be as small as possible.

An aggravating factor to the interception problem with a SHR is that there are situations when an emitter never transmits when the receiver is tuned to it's band. This is related to the periodic nature of both the emitter and the receiver, and the situation can occur continuously. This can also benefit the receiver in that if an intercept occurs, the periodic nature will cause it to continue occurring. This relationship is known as synchronization between the emitter and receiver.

The effects of synchronization are very difficult to analyze instinctively. With multiple emitters operating at different frequencies, with different scan rates, and different pulse repetition intervals, it is very difficult to choose the durations for a receiver schedule that provides 'good' intercept times, and to understand the effects of changing those durations.

2.4 Summary

The interception of radar signals is a fundamental task in ESM, and it is important that the maximum intercept time to intercept an emitter be known. The radar emitter characteristics of interest are:

- All emitters have a periodic scan defined by: the RF frequency of transmission F, the scan period T_{scan}, the scan duty cycle λ_{scan}, and the pulse repetition interval PRI.
- No emitter uses low probability of intercept techniques

- Scan rate is much larger than the pulse repetition interval
- Pulse repetition interval is much larger than the pulse width
- The scan duty cycle accounts for the exploitation of emitter side lobes and propagation effects
- All emitters have the same detection priority

The ESM receiver characteristics of interest are:

- The receiver is a scanning superheterodyne receiver with a fixed re-tuning time t_{tune}
- A receiver schedule consists of a set of durations, one for each frequency band
- The receiver must scan all the frequency bands
- The receiver has an omni-directional antenna
- The effects of receiver sensitivity and noise floor are not taken into account

The requirements necessary for an interception to occur are:

- The ESM receiver must be tuned to the frequency of transmission of the radar emitter at the time the transmission occurs;
- The radar system must be transmitting in the direction of the ESM receiver; and
- The receiver must receive a minimum number of pulses from the emitter.

Chapter 3

Maximum Intercept Time

Maximum intercept time is the maximum amount of time required for an ESM system to intercept a transmission from a radar emitter. While other indicators of ESM system performance are available (average time to intercept, probability of intercept based on listening time, etc.), the calculation of maximum intercept time provides a substantive measure of the level of threat to a military resource and can be considered as a factor in the planning of a mission. The other performance measures are important, but are calculated using stochastic techniques because of the unknown starting phase of the emitter transmission. These stochastic methods provide 'best estimate' values that complement the deterministic calculation of the maximum intercept time.

The calculation of maximum intercept time stems from the analysis of pulse trains, which are simply abstract descriptions of periodic behavior. The analysis of coincident pulse trains relies on the field of Number Theory. The coincidence of individual pulse trains is well understood, and several methods exist to quickly determine intercept time solutions.

This chapter proceeds in three sections. First, emitter and receiver parameters are mapped to their equivalent pulse train parameters. Secondly, the analysis of pulse trains using Number Theory is explained. This explanation starts with the case of trivial pulse trains and trivial coincidence (zero phase, integer-valued periods, and infinitely short pulse widths). Integer-valued phase differences are then introduced. Following this, non-trivial pulse trains and non-trivial coincidence are then examined (real-valued phases, periods, and pulse widths). Finally, the use of the maximum intercept time

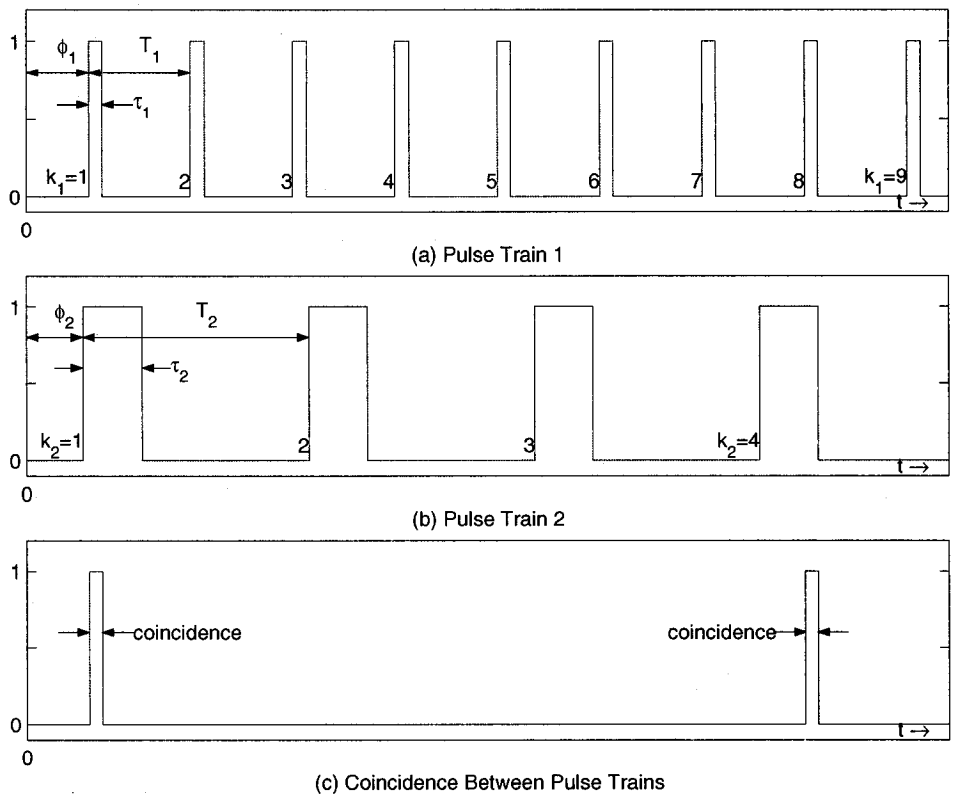

Fig. 3.1 Pulse Train Parameters where (a) could be an emitter and (b) could be a receiver. The coincidence between (a) and (b) is shown at (c).

calculations within the context of the ESM problem are explained.

3.1 Coincident Pulse Trains

The allocation of a scanning superheterodyne receiver to a particular frequency band and the transmissions from a radar emitter can each be described as a periodic pulse train. In general, pulse trains are described by their period (T_n), pulse width (τ_n), pulse index (k_n), and their starting phase (ϕ_n) (see Figure 3.1.

The emitter pulse train has a value of one when the emitter is transmitting pulses in the direction of the receiver. The length of the emitter scan corresponds to the length of the emitter pulse train pulse (τ_1 in Figure 3.1 is equivalent to λT from Figure 2.1). Note that the pulse of an emitter pulse train is not equivalent to the RF pulse transmitted by an emitter. The period of the emitter pulse train corresponds to the scan rate of

the emitter (T_1 in Figure 3.1 is equivalent to T_{scan} from Figure 2.1). When an emitter is not transmitting in the direction of the receiver, the emitter pulse train has a value of zero.

A receiver pulse train is determined with reference to a frequency band. When the receiver is allocated to the frequency band, it has a value of one (and zero otherwise). The length of the receiver pulse train pulse corresponds to the receiver schedule duration for the frequency band (d_m from Figure 2.2 is equivalent to τ_2 from Figure 2.1). The period of the receiver pulse train corresponds to the period of the receiver schedule (T_{sched} from Figure 2.2 is equivalent to T_2 from Figure 2.1). For a receiver that is scanning M frequency bands, M pulse trains are required to describe it.

When a pulse from both the receiver pulse train and an emitter pulse train occur at the same time, a coincidence occurs. If the coincidence contains the minimum required number of emitter pulses, an intercept occurs. The basis of the maximum intercept time analysis is to determine the first pulse from each pulse train which causes an intercept, which indicates the time at which the intercept will occur.

3.2 Coincident Pulse Train Analysis using Number Theory

Number Theory is the study of the properties of whole numbers [6], and is the basis of the calculation of pulse train coincidence. Starting with the analysis of trivial pulse trains with zero phase ($\phi_1 = \phi_2 = 0$), differing periods ($T_1 \neq T_2$, $T_1, T_2 \in \mathbb{N}$), and infinitely short pulses ($\tau_1 = \tau_2 = \delta$), the theory is modified to demonstrate how phase differences, real-valued periods, and non-negligible pulse widths affect the coincidence calculations.

3.2.1 Trivial Coincidence

The coincidence of pulses in trivial pulse trains is analogous to the concept of *common multiples*. The first coincidence of pulses (and hence the maximum intercept time) occurs between the pulses corresponding to the *least common multiple* (LCM) of the periods of the two pulse trains.

3.2.2 LCM, GCD, and Euclid's Algorithm

As detailed in the text by Ore [7], calculation of the LCM is straightforward: When a and b are two numbers with the greatest common divisor $d = (a, b)$, the least common multiple is:

$$[a, b] = \frac{ab}{d} \tag{3.1}$$

The problem then becomes one of determining the *greatest common divisor* (GCD) of the periods of the two pulse trains. Euclid's algorithm is an effective means of finding the GCD between two numbers a and b: Assuming a and b are positive and $a > b$, divide a by b with respect to the least positive remainder:

$$a = q_1 b + r_1, \quad 0 \leq r_1 < b$$

Then divide b by r_1

$$b = q_2 r_1 + r_2, \quad 0 \leq r_2 < r_1$$

And continue these steps until $r_{n+1} = 0$

$$\begin{aligned} r_1 &= q_3 r_2 + r_3 \\ &\cdots \\ r_{n-2} &= q_n r_{n-1} + r_n \\ r_{n-1} &= q_{n+1} r_n \end{aligned} \tag{3.2}$$

The last non-vanishing remainder r_n corresponds to the GCD of a and b.

3.2.3 Diophantine Equations and Euclid's Algorithm

Calculating the LCM is useful for trivial coincidence, but as we start to analyze the non-trivial case, the use of Diophantine equations provides a useful analytical tool. The general form of the Diophantine equation is:

$$ax - by = c \tag{3.3}$$

where a and b ($a, b \in \mathbb{N}$) represent the periods (T_1, T_2), and c represents the phase difference of the two pulse trains, expresses the coincidence between the xth pulse of pulse train 1 and the yth pulse of pulse train 2 ($x, y \in \mathbb{N}$).

Solutions to Diophantine equations have been studied extensively, and referring again to Ore [7], a solution only exists when the GCD of a and b divides c. When this is the case and equation 3.3 is divided by the GCD $d = (a, b)$, a and b are relatively prime (they share no common factors other than 1), so the solution to

$$ax_0 - by_0 = 1 \tag{3.4}$$

can be multiplied by c to find

$$a(cx_0) - b(cy_0) = c \tag{3.5}$$

resulting in

$$x = cx_0 \quad \text{and} \quad y = cy_0 \tag{3.6}$$

The solution to equation 3.4 can be found by extending Euclid's algorithm. Modifying the notation to use $a = r_1$ and $b = r_2$, from equation 3.2 we have

$$\begin{aligned} r_1 &= q_1 r_2 + r_3 \\ r_2 &= q_2 r_3 + r_4 \\ &\dots \\ r_{n-3} &= q_{n-3} r_{n-2} + r_{n-1} \\ r_{n-2} &= q_{n-2} r_{n-1} + 1 \end{aligned} \tag{3.7}$$

The last remainder will always be 1 since a and b are relatively prime. The values for x_0 and y_0 can be found by unwinding the solution. Rearranging the last equation from 3.7,

$$1 = r_{n-2} - q_{n-2}r_{n-1} \tag{3.8}$$

and substitute for previous values of r

$$\begin{aligned} & r_{n-1} = r_{n-3} - q_{n-3}r_{n-2} \\ \rightarrow \quad & 1 = -q_{n-2}r_{n-3} + (1 + q_{n-2}q_{n-3})r_{n-2} \\ & \ldots \end{aligned} \tag{3.9}$$

until $r_1 = x_0$ and $r_2 = y_0$ have been substituted and we have the solution to equation 3.4 (and 3.5).

Euclid's algorithm will be of great assistance when mathematically calculating the effects of synchronization and coincidence in the following sections.

3.2.4 Synchronization

Synchronization is a term used to describe the relationship between two pulse trains. Because of the periodic nature of the pulses, each pulse train is locked, or synchronized to the other. If a coincidence occurs, it will continue to occur regularly. If no coincidence occurs, it will never occur. Miller and Schwarz [8] used the theory of linear congruences to analyze the effect of synchronization and demonstrate when coincidence occurs. This theory accounts for the effects of differing phase ($\phi_1 = 0, \phi_2 \in [0, T_2)$) between two pulse trains with integer-valued periods ($T_n \in \mathbb{N}$). The following is a summary of the theory using [8] and [7]:

Two integers a and b are *congruent for the modulus* m when their difference $a - b$ is divisible by the integer m. This is expressed as

$$a \equiv b \pmod{m} \tag{3.10}$$

When a and b are not congruent, they are called *incongruent for the modulus* m

$$a \not\equiv b \pmod{m} \tag{3.11}$$

A *linear congruence* is a congruence of the form

$$ax \equiv b \pmod{m} \tag{3.12}$$

where the problem is to find an integer x such that $ax - b$ is divisible by m. From the definition of *congruency*, we can re-write this as

$$ax - b = my$$

or

$$ax - my = b \tag{3.13}$$

From section 3.2.3, we know that this is only solvable if the GCD $d = (a, m)$ divides b. When a and m are relatively prime, there is a single solution where x and y can be found using Euclid's algorithm. This relates directly to the coincidence between pulse trains - when the congruence has a solution, coincidence will occur - when the congruence does not have a solution, no coincidence will occur. The ratio of the two values x and y are said to form a *synchronization ratio.*

When one solution of a linear congruence has been determined, other solutions (corresponding to the regularly occurring coincident pulses) can be found by using the LCM (a, m). If x_0 is the smallest non-negative solution to equation 3.10, then $x_0 + x'$ is also a solution where

$$ax' = LCM(a, m) \tag{3.14}$$

By substituting $x_0 + x'$ into equation 3.10, we obtain

$$\begin{aligned} &a(x_0 + x') - b \\ &= (ax_0 - b) + ax' \equiv 0 \pmod{m} \end{aligned} \tag{3.15}$$

since m divides $(ax_0 - b)$ (by the congruence solution)and m also divides ax' (by the LCM).

No solutions can exist between x_0 and $x_0 + x'$ from the following. If a solution $x_0 + x''$ did exist, such that

$$x_0 < x_0 + x'' < x_0 + x' \tag{3.16}$$

then the following must hold true (by substituting as we did previously):

$$a(x_0 + x'') - b$$

$$= (ax_0 - b) + ax'' \equiv 0 \pmod{m} \tag{3.17}$$

The first part holds true since m divides $(ax_0 - b)$, but the second is false because both a and m must divide ax'', but there is no number lower than $ax' = LCM(a, m)$ where this is possible.

The use of linear congruences has allowed us to calculate if coincidences occur, how they will continue to re-occur, and how it is possible that coincidences may not occur.

3.2.5 Non-Trivial Coincidence

The examination of the trivial coincidence of pulses has shown how number theory is useful in calculating the maximum intercept time. However, for these calculations to be useful, we must expand the analysis and incorporate real-valued periods ($T_n \in \mathbb{R}$), real-valued phase difference ($\phi_n \in [0, T_n)$), finite pulse widths ($\tau_n \in \mathbb{R}$, $\tau_n < T_n$), and a minimum overlap between pulses. Each of these complicates the coincidence analysis, but the solution relies on that portion of number theory that studies integer approximations to real-valued numbers.

3.2.6 Homogeneous Diophantine Approximation

Homogeneous Diophantine approximation is the practice of finding two integers p and q such that

$$|q\alpha - p| < \epsilon \tag{3.18}$$

where α and ϵ are real-valued.

The *best approximation* of p and q can be defined in several ways, but we will use the definition described by Clarkson [9]. The fraction p/q, $q > 0$ is a best approximation to α if, for all other fractions p'/q', $q' > 0$,

$$q' \leq q \Rightarrow |q'\alpha - p'| \geq |q\alpha - p| \tag{3.19}$$

and

$$|q'\alpha - p'| \leq |q\alpha - p| \Rightarrow q \leq q' \tag{3.20}$$

which means that the best approximation will be that fraction p/q with the lowest-valued denominator that gives an error on $|q\alpha - p|$ of less than ϵ. The ratio of the two values p and q form a synchronization ratio.

3.2.7 Simple Continued Fractions

The *simple continued fraction* (s.c.f) is a means of expressing any real number in fractional form. For any real number $\alpha \geq 0$, the s.c.f. has the form

$$\alpha = a_0 + \cfrac{1}{a_1 + \cfrac{1}{a_2 + \cfrac{1}{a_3 + \cdots}}} \tag{3.21}$$

where $a_n \in \mathbb{N}$ for $n > 0$ and $a_0 \geq 0$. The values a_n are called the *partial quotients* and the value of the s.c.f truncated after n partial quotients is called the *nth convergent of the s.c.f.*.

The characteristics of the s.c.f have been well studied, and in the context of this work it is important to note the following properties (from Clarkson et al [10]):

- if α is rational, ($\alpha \in \mathbb{Q}$), the s.c.f. terminates. If α is not rational ($\alpha \notin \mathbb{Q}$), the s.c.f. does not terminate.
- the fractions p_n/q_n generated by the nth convergents of the s.c.f are *best approximations* of α (see equations 3.19 and 3.20) and provide solutions to homogeneous Diophantine approximations of the form in equation 3.18
- The convergents of the s.c.f. can be calculated using variations of Euclid's algorithm.

3.2.8 The Farey Series

The Farey series F_n is the set of irreducible rational numbers a/b with $0 \leq a \leq b \leq n$ and the LCM$(a, b) = 1$ arranged in increasing order [6]. For example, the Farey series

up to order $n = 5$ is

$$\begin{aligned} F_1 &= \left\{\frac{0}{1}, \frac{1}{1}\right\} \\ F_2 &= \left\{\frac{0}{1}, \frac{1}{2}, \frac{1}{1}\right\} \\ F_3 &= \left\{\frac{0}{1}, \frac{1}{3}, \frac{1}{2}, \frac{2}{3}, \frac{1}{1}\right\} \\ F_4 &= \left\{\frac{0}{1}, \frac{1}{4}, \frac{1}{3}, \frac{1}{2}, \frac{2}{3}, \frac{3}{4}, \frac{1}{1}\right\} \\ F_5 &= \left\{\frac{0}{1}, \frac{1}{5}, \frac{1}{4}, \frac{1}{3}, \frac{2}{5}, \frac{1}{2}, \frac{3}{5}, \frac{2}{3}, \frac{3}{4}, \frac{4}{5}, \frac{1}{1}\right\} \end{aligned} \tag{3.22}$$

Clarkson [9] showed that the Farey Series of the appropriate order provides a convenient method for enumerating all the best approximations p/q of a real number α for a given approximation error $\eta = q\alpha - p$. These best approximations correspond to the convergents of the s.c.f. and the related solutions to homogeneous Diophantine equations.

The *Augmented, Generalized Farey Series* $\mathfrak{G}^*(\lambda_1, \lambda_2)$ was defined by Clarkson [11] where each element corresponds to a synchronization ratio between two pulse trains with duty cycles λ_1 and λ_2. Algorithm 3.1 and 3.2 are the recursive algorithms used to generate the series:

For instance, the complete augmented, generalized Farey Series for $\lambda_1 = 0.13$ and $\lambda_2 = 0.26$ is

$$\mathfrak{G}^* = \left(\frac{0}{1}, \frac{1}{5}, \frac{1}{4}, \frac{1}{3}, \frac{1}{2}, \frac{2}{3}, \frac{1}{1}, \frac{2}{1}, \frac{3}{1}, \frac{1}{0}\right) \tag{3.23}$$

3.2.9 Phase Difference and Pulse Overlap

Determining the effect of a phase difference on the coincidence between two pulse trains was first investigated by Richards [12], and subsequently by Miller and Schwarz [8], and Friedman [13]. Kelly et al [14], Clarkson et al [10], and Clarkson [9] approached the problem with a desire to calculate the mean probability of intercept between pulse trains. The results of this work demonstrated that if the phase (ϕ_1) of one pulse train

input : $(k, h, k', h', \lambda_1, \lambda_2)$, where h/k and h'/k' are the left and right starting elements of the series and λ_n are the duty cycles for pulse train n
output: $\mathfrak{G}$, the list of Generalized Farey Series elements

```
1 proc 𝔊 = genfarey(k, h, k', h', λ1, λ2):
2 begin
3     𝔊 = [];
4     if λ1(k + k') + λ2(h + h') < 1 then
5         𝔊 = 𝔊 + genfarey(h, k, h + h', k + k', λ1, λ2);
6         𝔊 = 𝔊 + (h + h')/(k + k');
7         𝔊 = 𝔊 + genfarey(h + h', k + k', h', k', λ1, λ2);
8 end
```

Algorithm 3.1: Producing the Generalized Farey Series

input : $(k, h, k', h', \lambda_1, \lambda_2)$, where h/k and h'/k' are the left and right starting elements of the series and λ_n are the duty cycles for pulse train n
output: $\mathfrak{G}^*$, the list of Augmented, Generalized Farey Series elements

```
1 proc 𝔊* = augfarey(k, h, k', h', λ1, λ2):
2 begin
3     𝔊* = [0/1];
4     𝔊* = 𝔊* + genfarey(h, k, h', k', λ1, λ2);
5     𝔊* = 𝔊* + [1/0];
6 end
```

Algorithm 3.2: Producing the Augmented, Generalized Farey Series

was assumed known (and one normally is known in ESM applications - that of the ESM receiver), the pulse overlap from a second pulse train could be analyzed with reference to the period of the first pulse train, and that an expression could be found indicating when a coincidence would occur (or not), independent of the starting phase of the second pulse train.

Formulating the problem as a Diophantine approximation, they defined $\alpha = T_2/T_1$ and $\epsilon = \Delta/T_1$ where Δ is the minimum duration required for coincidence to occur. With β as the unknown phase of pulse train 2, an approximate coincidence occurs between the p_Nth pulse of pulse train 1 and the q_Nth pulse of pulse train 2 when

$$|q_N\alpha - p_N - \beta| \leq \epsilon \tag{3.24}$$

The expression that Clarkson [9] derived stated that the maximum number of pulses from the second pulse train (N) before an intercept occurs is

$$N = \begin{cases} \infty & \text{if } |\eta_N| = 0, \\ q_{N+1} + q_N - kq_N & \text{if } |\eta_N| \neq 0. \end{cases} \tag{3.25}$$

where the approximation error $\eta_N = q_N\alpha - p_N$, the value k is calculated as

$$k = \left\lfloor \frac{\epsilon - |\eta_{N+1}|}{|\eta_N|} \right\rfloor, \tag{3.26}$$

p_N/q_N is the Nth convergent of α, and p_{N+1}/q_{N+1} is the $(N+1)$th convergent of α.

In the case when $|\eta_N| = 0$, the s.c.f. of α terminates because $\alpha \in \mathbb{Q}$, corresponding to a synchronization between the two pulse trains where coincidence may not occur.

3.2.10 Calculating Maximum Intercept Time

All the theory has now been laid out to allow the calculation of maximum intercept time from the non-trivial coincidence of two pulse trains. Clarkson [11] formulated the problem as follows:
From Figure 3.1, a pulse occurs at all times t when

$$|t - k_1T_1 - \phi_1| \leq \tfrac{1}{2}\tau_1 \tag{3.27}$$

where t is time, and k_1, T_1, ϕ_1, and τ_1 are all similarly defined as in Figure 3.1. Coincidence between two pulse trains occurs when both pulses occur simultaneously

$$|(k_1T_1 + \phi_1) - (k_2T_2 + \phi_2)| \leq \tfrac{1}{2}(\tau_1 + \tau_2) \tag{3.28}$$

Equation 3.28 allows for the accounting of pulse overlap. If a minimum overlap of duration d is required for coincidence to occur, then the pulse width values (τ_1 and τ_2) can each be reduced by the duration D of the overlap. If either τ_n is less than D then the minimum duration required of the coincidence will not occur.

$$|(k_1T_1 + \phi_1) - (k_2T_2 + \phi_2)| \leq \tfrac{1}{2}(\tau_1 + \tau_2 - D),\ \tau_1, \tau_2 \geq D \tag{3.29}$$

In order to analyze the non-trivial coincidence problem with the theory developed in the previous sections, it is useful to define the *ratio of PRIs*

$$\alpha = \frac{T_2}{T_1}, \tag{3.30}$$

the *normalized sum of pulse widths*

$$\epsilon = \frac{\tau_1 + \tau_2}{T_1}$$

where the duty cycles

$$\lambda_1 = \frac{\tau_1}{T_1} \text{ and } \lambda_2 = \frac{\tau_2}{T_2}, \text{resulting in}$$

$$\epsilon = \lambda_1 + \lambda_2\alpha \tag{3.31}$$

and the *normalized phase difference*

$$\beta = \frac{\phi_2 - \phi_1}{T_1}. \tag{3.32}$$

Substituting these values into equation 3.28 and setting $k_1 = p$ and $k_2 = q$ results in

$$|q\alpha - p + \beta| \leq \tfrac{1}{2}\epsilon. \tag{3.33}$$

which is in the form of an inhomogeneous Diophantine approximation.

Clarkson [11] devised Algorithm 3.3 for generating the maximum intercept time by observing that we can remove the phase difference β by using the pulse overlap calculations and determining the values for p and q by enumerating the Farey Series of the correct order.

input : $(T_1, T_2, \lambda_1, \lambda_2)$, where T_n is the PRI and λ_n are the duty cycles for pulse train n
output: t, the maximum intercept time

proc t = intercepttime$(T_1, T_2, \lambda_1, \lambda_2)$): ;
begin
  Calculate the ratio of PRIs, α, according to equation 3.30;
  Calculate the augmented, generalized Farey Series $\mathfrak{G}^*(\lambda_1, \lambda_2)$;
  From $\mathfrak{G}^*(\lambda_1, \lambda_2)$, locate the adjacent pair of elements $h/k < h'/k'$ that surround α;
  if $\alpha = h/k$ ***or*** $\alpha = h'/k'$ **then**
    $t = \infty$
  else
    if $k < k'$ **then**
      $$x = \frac{h + \lambda_1}{k - \lambda_2}$$
    else
      $$x = \frac{h' - \lambda_1}{k' + \lambda_2}$$
    end
    if $\alpha < x$ ***or*** $(k < k'$ ***and*** $\alpha = x)$ **then**
      $(p, q, P, Q) = (h, k, h', k')$
    else
      $(p, q, P, Q) = (h', k', h, k)$
    end
    $$\kappa = \left\lfloor \frac{\epsilon - |Q\alpha - P|}{|q\alpha - p|} \right\rfloor;$$
    $t = T_2(Q + q - \kappa q)$;
  end
end

Algorithm 3.3: Intercept Time for Constant Duty Cycles

Figure 3.2 clearly demonstrates the effects of the synchronization ratios (as described in 3.23) and was created using Algorithm 3.3 with the values $\lambda_1 = 0.13$, $T_1 = 1$,

$\lambda_2 = 0.26$, and T_2 changes from 0.1 to 4 (values taken from [11]). The effects of the synchronization ratios are clear as the maximum intercept time increases to infinity for the values as specified by the Farey Series at 3.23.

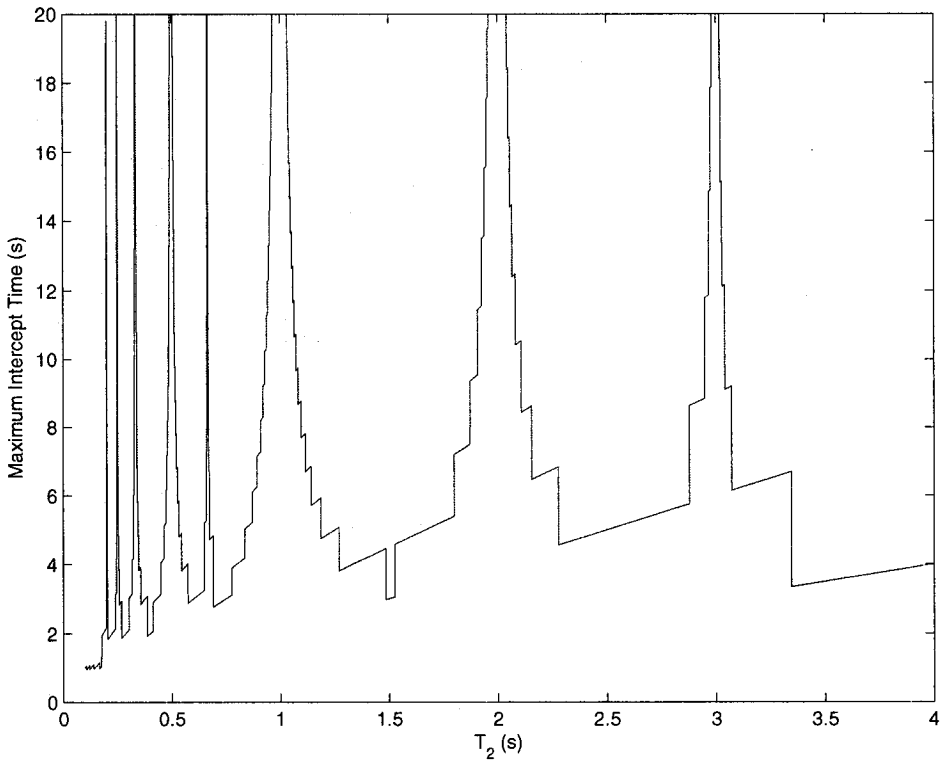

Fig. 3.2 Maximum Intercept Time for Two Pulse Trains

3.3 ESM Context

The ESM application of interest involves the use of a scanning super-heterodyne receiver (SHR) to search for multiple radar emitters spread across multiple frequencies. The previous section has outlined the theory that allows us to calculate the maximum intercept time between two pulse trains, but the question still remains of how this can be utilized.

We know that the SHR (by its nature) must scan through the spectrum of interest in a series of discrete frequency bands. It dwells on each band for a period of time defined by the receiver schedule. Each band may contain many, one, or no radar emitters of interest. For each emitter that does transmit in a particular frequency band m, we can use Algorithm 3.3 to calculate the maximum intercept time by setting

$$\begin{aligned} \lambda_1 &= \lambda_{scan_n} = \text{the scan duty cycle of emitter } n \\ T_1 &= T_{scan_n} = \text{the scan PRI of emitter } n \\ \lambda_2 &= \frac{d_m}{T_2} = \text{the duty cycle of duration m} \\ T_2 &= T_{sched} = \left(\sum_{m=1}^{M} d_m \right) + M(t_{tune}) \end{aligned} \tag{3.34}$$

where the emitter n is transmitting in frequency band m, d_m is the duration the SHR is tuned to frequency band m, M is the total number of SHR tuning bands, and t_{tune} is the time required for the SHR to tune to another frequency band. The duration d_m must exceed the minimum time required to intercept emitter n (normally a fixed number of radar pulses).

From equation 3.34, any change to a duration d_m affects the total SHR period T_2. Figure 3.2 shows that any changes to these variables has a non-linear impact on the maximum intercept time, that the maximum intercept time function is non-monotonic, and that there are multiple minima. If we want to minimize the maximum intercept time for an emitter, then we need to choose d_m accordingly. However, varying any d_m changes T_2, and hence the maximum intercept time for every other $(N-1)$ emitters could also change.

If we naively adjust consecutive d_m values, we may or may not find values that pro-

vide acceptable maximum intercept times. A global optimization technique, however, should be able to examine all the d_m variables simultaneously, and choose appropriate values that do not conflict with each other.

3.4 Summary

The calculation of the maximum intercept time between a scanning super-heterodyne receiver (S.H.R) and a radar emitter requires the problem to be formulated as a co-incidence between two pulse trains. This type of coincidence is well understood, and algorithms that rely heavily on the field of Number Theory have been developed by Clarkson et al to produce solutions to the non-trivial case. The ESM context requires that the SHR scan for multiple emitters which may transmit in different frequency bands of the receiver. Creating a schedule for the SHR that reduces the maximum time to intercept for each of these emitters is difficult because of the non-linear nature of the maximum intercept time function, and the interdependency of the SHR durations in each scanned frequency band. The use of a global optimization technique is the proposed solution to these problems, and is investigated in the following chapters.

Chapter 4

Resource Allocation for ESM Receivers

The interception of a pulsed radar emitter by a scanning super-heterodyne receiver (SHR) can be modeled as the coincidence between two pulse trains, and the mathematics used to calculate the maximum intercept time were presented in the previous chapter. But knowing how to calculate the maximum intercept time does not explain how the receiver parameters should be set. The SHR is a resource whose purpose is to intercept multiple emitters which are transmitting across multiple frequency bands, and we want to generate a schedule for the receiver that intercepts each emitter in the shortest possible time frame. The generic problem of the 'fair allocation of scarce resources' has been studied extensively, and in this chapter we will examine several possible techniques for setting the receiver parameters to generate a receiver schedule.

Before examining the details of schedule generation, it is important to specify several desirable properties of any chosen generation technique. Firstly, any technique must address the parameter generation problem from a systematic approach and account for the effect of the values of all variables simultaneously. Any schedule that is created must be tested against the emitters of interest and its performance must be measured in a repeatable fashion. The performance of the schedule relies on the maximum intercept time calculations, so the technique must be capable of implementing the theory outlined in the previous chapter.

4.1 Resource Scheduling Theory

The study of the many diverse areas of minimization and optimization is known as *Optimization Theory* [6]. By evaluating a problem with a scientific approach, it is possible to describe a problem as a mathematical model and apply various known algorithms to generate solutions [15].

In order to be successful, the various algorithms can only be applied to mathematical models that have certain properties. Some techniques, such as the simplex and interior point methods only apply when the variables interact in a linear fashion, while others such as gradient methods can account for non-linear effects. Some techniques can only deal with integer or binary valued variables, while others can handle those with real values. And some techniques can find an optimal solution, while others use heuristic techniques and can only find 'good' solutions that may be 'close' to an optimal one. Describing a particular problem as a mathematical model and finding 'the best' solution technique is an entire field of study, and no attempt is made here to survey the entire field or describe the state of the art. However, the maximum intercept time problem closely resembles other problems where scarce resources need to be shared in the best way possible, all the while accounting for other constraints. In order to examine the properties of our problem and investigate what techniques may be available to solve it, we need to construct the mathematical model that describes it.

4.2 Problem Formulation

The decision variables which are used to minimize the maximum intercept time are the durations that the super-heterodyne receiver (SHR) dwells in each frequency band. These durations are specified as

$$d_m, \quad m = 1..M \tag{4.1}$$

where m is the index of the frequency band and there are M frequency bands.

The objective function we are trying to minimize is the sum of the maximum intercept times for each emitter. The maximum intercept time provides a guaranteed measure of an intercept, and since each emitter has different parameters, the sum of all the maximum intercept times (for each emitter) is the best non-statistical performance

measurement.

$$Z = \sum_{n=1}^{N} (intercepttime(T_1, T_2, \lambda_1, \lambda_2))_n \tag{4.2}$$

where N is the number of emitters, $intercepttime(\dots)$ is the value returned by Algorithm 3.3, and the values $(T_1, T_2, \lambda_1, \lambda_2)$ are repeated from 3.34.

$$\begin{aligned}
\lambda_1 &= \lambda_{scan_n} = \text{the scan duty cycle of emitter } n \\
T_1 &= T_{scan_n} = \text{the scan PRI of emitter } n \\
\lambda_2 &= \frac{d_m}{T_2} = \text{the duty cycle of duration m} \\
T_2 &= T_{sched} = \left(\sum_{m=1}^{M} d_m \right) + M(t_{tune})
\end{aligned}$$

It should be noted that the value Z is the sum of each emitter's maximum intercept time, each of which is calculated *independent of phase*, which removes any phase dependency of the objective function.

The constraints to this problem are: the number of frequency bands M scanned by the SHR (of magnitude 10), the SHR re-tuning time t_{tune}(of magnitude 0.1 s), and the minimum duration d_m (which must exceed the minimum time $10(t_{pulsePRI}) \leq d_m$ for emitter n and be less than the maximum allowed duration $t_{MaxDuration}$). Additionally, the scan duty cycle, the scan PRI, and the pulse PRI of each emitter is known, but the starting phase (ϕ_n) of each emitter is not.

The fixed parameters of the emitters and the receiver are:

$$\begin{aligned}
&(\lambda_1, T_1, t_{pulsePRI}, \phi_n, t_{tune}) \in \mathbb{R} \\
&(T_1, t_{pulsePRI}, t_{tune}) > 0 \\
&0 < \lambda_1 < 1 \\
&\phi_n \in [0, T_1)
\end{aligned} \tag{4.3}$$

While the theory allows calculations using any positive, real-valued duration, practical implementation details of resolution in the SHR only allow a discrete number p

of duration values ($d_m \in \mathbb{Z}^p,\ d_m > 0$) where p is of the order 10^6 for microsecond resolution.

4.3 Choosing an Appropriate Optimization Technique

Now that we have a mathematical model of our problem, we need to investigate its properties in order to determine if a suitable algorithm or solution technique exists.

The objective function for the problem is non-linear. The relationship between the periods and starting phases of an emitter and a receiver was outlined in the previous chapter, and Figure 3.2 clearly shows the non-linear character of the intercept time. As defined in the previous section, the decision variables all hold discrete values, so the algorithm must be able to handle these.

The complexity of the problem places a significant requirement on the choice of algorithm. The order of the problem is exponential, since the possible number of calculations required to find the best schedule is $O(D^M)$, where D represents the number of discrete values each duration d_m can hold, and M is the number of frequency bands being scanned. As the number of frequency bands is increased, the scheduling possibilities suffers from combinatorial explosion. The only reasonable techniques that are available to solve problems of this magnitude are those that rely on heuristic algorithms. These do not guarantee an optimal schedule, but generate schedules that may be close to the optimal. As a result of these conditions, we need to examine the available heuristic algorithms that can solve a non-linear, discrete-valued problem in a systematic and repeatable manner.

Method Name	Heuristic	Non-Linear	Discrete	Repeatable
Exhaustive Search	No	Yes	Yes	Yes
Genetic Algorithms	Yes	Yes	Yes	Yes
Gradient Methods	No	Yes	Yes	Yes
Greedy Search	Yes	Yes	Yes	Yes
Hooke and Jeeves	Yes	Yes	Yes	Yes
Simulated Annealing	Yes	Yes	Yes	Yes
Tabu Search	Yes	Yes	Yes	Yes

Table 4.1 Properties of Several Optimization Techniques

There are many optimization methods that meet most of these criteria, a selection

of which are listed in Table 4.1. We can see that most of the methods can be applied to the receiver scheduling problem, but for implementation reasons, genetic algorithms were chosen as the optimization technique.

4.3.1 Genetic Algorithms

Genetic algorithms (GA) are optimization techniques that follow a sequence of steps inspired by the biological evolution of species in the natural world [16]. They are a heuristic technique that have proven themselves very useful at spanning a search space in a computationally efficient manner. Since their inception, GAs have taken many variations and have been specialized for specific applications, but the basic steps of the algorithm are outlined in Algorithm 4.1.

```
1  begin
2      Choose the initial population of individuals;
3      Calculate the fitness of each individual in the population;
4      repeat
5          Use a reproduction operator to randomly select from the best individuals;
6          Use a crossover operator to generate and breed new individuals;
7          Use a mutation operator to randomly change the values of randomly
           selected individuals;
8          Calculate the fitness of each individual in the population;
9      until terminating conditions met;
10 end
```

Algorithm 4.1: Genetic Algorithm

Goldberg [17] provides guidance on how to promote successful use of genetic algorithms, which are outlined in the following items and are addressed in the next chapter:

- **Initial Population**. All GAs require that the decision variables be encoded as an artificial chromosome in a string/list format, and typically use fixed length strings. As with any optimization routine, if the initial population contains initial parameters that are close to a good solution, the GA will be much more successful at finding the good solution. The initial solution must provide a population large enough and with enough diversity to allow the GA to span the search space.

- **Fitness Function**. The fitness function provides a means of measuring the quality, or fitness of one individual against another. Since the construction of future generations depends on the sub-components (the genes or building-blocks) of an individual, it is important that it be designed to not deceive the GA (i.e. lead the algorithm away from the good solution), and that it provide suitable scaling among its individual parameters so that it is possible to safely compare one individual with another.

- **Reproduction Operator**. The reproduction operator must select the best individuals from the current population for use by the crossover operator. It must make these selections in such a way that future generations are able to successively improve their fitness values (i.e. selecting only one individual for crossover, even if it is the best one, will cause the optimization to stall, much as inbreeding can have detrimental effects in biological systems).

- **Crossover Operator**. The crossover, or recombination operator acts on two individuals to create a 'child'. There are many variations on how to do this, but they all involve the random selection of elements from the two 'parents' which are combined to form the 'child'. The crossover operator is important because it allows the algorithm to 'jump' to a different portion of the search space, preventing it from becoming trapped in a local minima. Elitism, where a number of the best solutions are kept from generation to generation, can be used in conjunction with the crossover operator. The crossover fraction defines the percentage of the population (other than elites) that are formed by the crossover of two parents. The remaining fraction (1 - the crossover fraction) defines how many children will be formed by mutation.

- **Mutation Operator**. The mutation operator acts on a randomly selected individual from the population to create a mutated 'child'. As with the reproduction operator, there are many variations on how to do this, but they all involve random changes to randomly selected elements of the individual chosen for mutation. The mutation operator allows exploration of the search space in the vicinity of a current solution.

- **Terminating Conditions**. The terminating conditions are the set of conditions

that controls when the GA stops iterating. The algorithm should stop when the optimal solution is found, but since there is no guarantee of optimality, other conditions need to be set. These limits are typically either

- the number of generations;
- the amount of processing time;
- obtaining a pre-determined fitness level; or
- when the incremental improvement of the fitness between generations is below a pre-determined level.

4.4 Pseudo-Random Scheduler

In order to compare the results of the genetic algorithm optimization technique, a naive pseudo-random (PR) scheduling technique was chosen. The PR scheduler worked by iterating through each frequency band, dwelling in that band for a randomly generated duration. This effectively created a pulse train that was the superposition of multiple random pulses. This random pulse train was then compared with the pulse train of each emitter, and an intercept occurred when there was a coincidence between pulses.

The PR method was chosen for comparison because it avoided synchronization with the emitter by not having any periodicity in its pulses. It did not rely on the maximum intercept time theory specified in previous chapters, and thus provided an impartial reference for comparison with the GA results. The main drawback of the PR method was that it required enumeration of the pulse trains to determine coincidence, which made the simulations very computationally intensive. The PR method does not provide a guaranteed maximum intercept time.

4.5 Summary

Creating a schedule for a super-heterodyne receiver that minimizes the maximum intercept time for multiple emitters, each of which radiates in multiple frequency bands, is a case of the generic optimization problem of 'the fair allocation of scarce resources'. By constructing a mathematical model of the problem, several optimization techniques were examined for their applicability. The complexity of the problem is of an exponential order, the objective function is non-linear, and the decision variables are discrete, and genetic algorithms was selected as the optimization technique. The problem remains to determine experimentally if genetic algorithms are able to create a useful receiver schedule for the maximum intercept time problem.

Chapter 5

Experimental Setup and Results

In this experiment, we used two techniques to generate schedules for scanning superheterodyne receivers (SHR): a genetic algorithm (GA) and a pseudo-random (PR) algorithm. A procedure was developed for generating receiver schedules, and multiple scenarios were created to examine the effects of differing combinations of emitters. Initial results from the GA technique allowed it to be improved by using the maximum-scan values, and a maximum-scan (MS) algorithm was created. The results for each scenario were then evaluated against the other scheduling techniques.

5.1 Procedure

Emitter and receiver models were created, and the parameters of these models were fed into each scheduler. The first used the GA approach and the second used a pseudo-random approach. Multiple scenarios were run multiple times, and the results from each run were recorded in separate log files. The GA scheduler produced a set of durations, and these values were used with the emitter parameters to generate a set of maximum intercept times. The pseudo-random scheduler produced maximum intercept times directly. Once all the values were available, the results were compared and the performance of each schedule was measured.

The schedulers were created using Matlab 6 (Release 13SP1) with the Genetic Algorithm and Direct Search Toolbox (Version 1.0). All processing was done using Microsoft Windows 2000 Server on 8 Dell PowerEdge 1750 servers, each installed with dual 2.8 GHz Intel Xeon processors and 512MB of memory.

5.1.1 Emitter and Receiver Models

Emitter and receiver models were created that contained representative parameters for a generic scanning superheterodyne receiver and generic pulsed radar emitters. The receiver model was created using the parameters outlined in Table 5.1, and the same receiver model was used in each scenario. The receiver had a single channel. The emitter models were created using the parameters outlined in Table 5.2, and different emitter models were used in each scenario. Each emitter had a single mode. Multiple emitter models were generated using normally distributed values within the ranges specified in Table 5.2, with the condition that a minimum of 10 RF pulses must be transmitted in each emitter scan. This condition ensured the possibility of coincidence between the receiver and the emitter (if there were less than 10 RF pulses, interception would never occur). The same models were used for consecutive runs of each scenario.

Parameter	Description	Value
t_{tune}	The time required for the receiver to change between frequency bands	0.1 s
BW_{inst}	The instantaneous bandwidth of the receiver	500 MHz
$F_{MinScan}$	The minimum center frequency which the receiver can scan	1 GHz
$F_{MaxScan}$	The maximum center frequency which the receiver can scan	25 GHz
$t_{MaxDuration}$	The maximum duration which the receiver will dwell on any frequency band	20 s
.	Minimum Pulses required for a feasible interception	10

Table 5.1 Description of the Receiver Model

Parameter	Description	Min Value	Max Value
F	The RF frequency of transmission	1 GHz	25 GHz
PRI	The pulse repetition interval	1.4ms	5.6 ms
T_{scan}	The scan period	1 s	12 s
λ_{scan}	The scan duty cycle	0.001	0.1
	Minimum scan width ($\tau = \lambda T$) for feasible interception	$\lambda T > 10 t_{pulsePRI}$	

Table 5.2 Description of the Emitter Model

5.1.2 Scenarios

In order to examine the effectiveness of the schedulers in generating schedules, four scenarios were created (Table 5.3). The first scenario, SESB, was a trivial scenario that allowed observation of the scheduler under simple conditions. The next two scenarios, SEMB and MESB, were slightly more complicated in that they contained multiple emitters. The last scenario, MEMB100, contained quantities and a distribution of emitters approaching that of reality.

Each scenario consisted of different quantities and distributions across frequency bands of emitters, and each scenario used the same receiver model. The actual parameters used in each scenario are listed in the appendix.

Scenario Name	No. of Emitters	Emitter Distribution
Single Emitter - Single Band (SESB)	1	1 band
Single Emitter - Multiple Bands (SEMB)	10	10 bands, each emitter separated onto 10 different frequency bands
Multiple Emitter - Single Band (MESB)	10	1 band, all emitters on the same frequency band
Multiple Emitter - Multiple Bands (MEMB100)	100	all emitters randomly (uniformly) distributed across all frequency bands

Table 5.3 Scheduling Scenarios

5.2 Measuring Performance

Measuring the performance of each schedule needed to be done in a consistent and repeatable fashion. To assist with this, the following definitions were used to express the quality of particular receiver schedules.

- "Emitter Intercept Time" is defined as the maximum intercept time for a particular emitter evaluated using a receiver schedule.
- "Schedule Intercept Time" is defined as the sum of the emitter intercept times for each emitter evaluated using a receiver schedule, and is simply the objective function Z from the previous chapter.

- A "Feasible Schedule" is defined as a schedule that produces a finite maximum intercept time for every emitter.

The results between the schedule intercept time for each scheduler was compared. The minimum, maximum, and mean emitter intercept times from each scheduler were also compared.

5.3 Genetic Algorithm Scheduler Setup

As outlined in the previous chapter and Goldberg [17], the initial population, fitness function, and operators of the genetic algorithm must be chosen carefully. In order for the algorithm to be successful, each needed to be tailored to the formulation of the problem.

5.3.1 Initial Population

The effects of the population size were examined by iterating through the GA with population sizes of 50 to 500 and plotting the results (Figure 5.1). No significant effects on the rate of minimization or the final result were observed, but the time to compute the fitness function for each generation increased as the population size increased. A reasonable run-time for each generation was obtained using a population size of 100.

The initial population was generated by picking initial durations that were uniformly distributed between a minimum and maximum value. The minimum duration value was the time required for coincidence of $10t_{pulsePRI}$ using the minimum $t_{pulsePRI}$ value from all the emitters. The maximum duration value was set at 20 s, an arbitrary value that exceeded all the emitter scan rates. Using these values provided the GA with a solution that contained reasonable starting values.

The genome size was set to 49. This corresponded with the number of frequency bands of the SHR required to span the required frequency range, defined in chapter 2 as:

$$\begin{aligned} M &= \frac{F_{MaxScan} - F_{MinScan} + BW_{inst}}{BW_{inst}} \\ &= \frac{25\text{GHz} - 1\text{GHz} + 500\text{MHz}}{500\text{MHz}} = 49 \end{aligned}$$

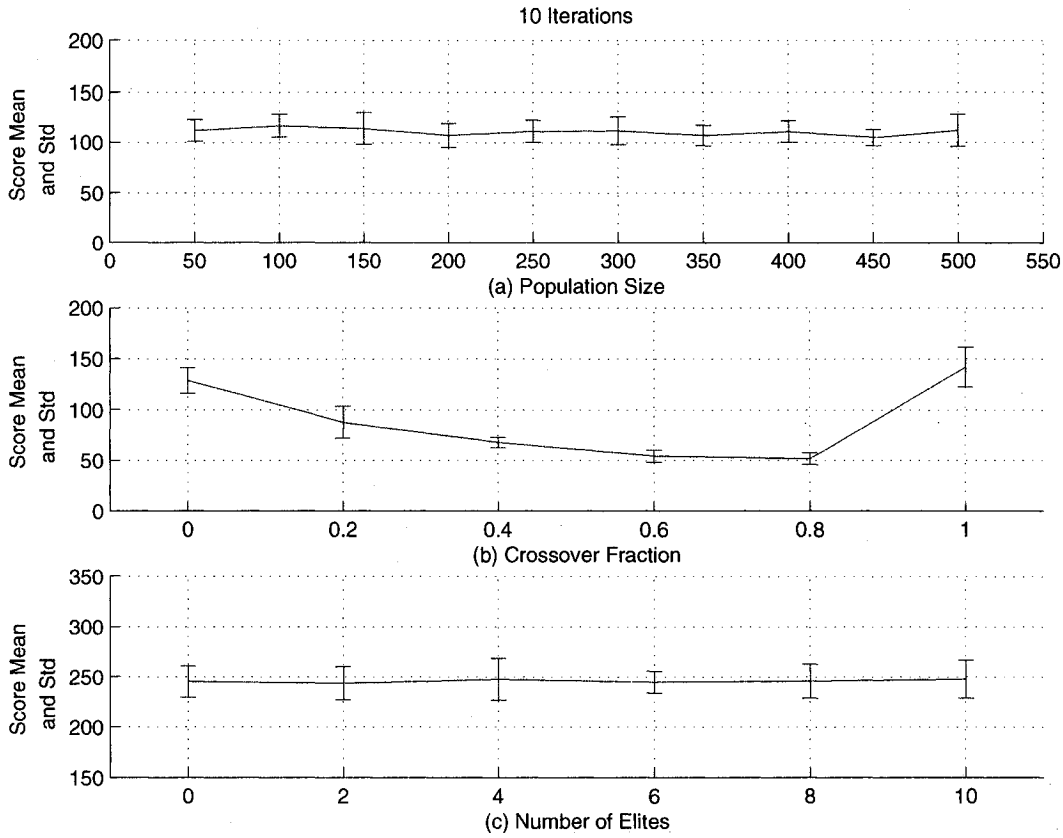

Fig. 5.1 The effects of several GA parameters on the Fitness Function Scores after 10 generations (Monte-Carlo summary for 10 iterations)

5.3.2 Fitness Function

The "Schedule Intercept Time" was used as the measure of the fitness. This was previously defined as the objective function at equation 4.2, but required slight modification in order to provide results in a reasonable time. The calculation of the fitness value was very processor intensive, and every effort was made to shorten the required number of calculations.

The resulting fitness function was

$$Z = \sum_{n=1}^{N} (intercepttime2(T_1, T_2, \lambda_1, \lambda_2))_n \tag{5.1}$$

where N is the number of emitters, $intercepttime2(\dots)$ is the value returned by Algorithm 5.2, and the values $(T_1, T_2, \lambda_1, \lambda_2)$ are repeated the same as those from Eq. 3.34.

Enumerating the Synchronization Ratios

The algorithm for generating the augmented, generalized Farey Series (Algorithm 3.2) has two limitations when used to enumerate the synchronization ratios:

1. The recursive nature of the algorithm results in an excessive use of computing stack; and

2. The algorithm returns all the elements of the augmented, generalized Farey Series of the appropriate order, when only the adjacent elements h/k and h'/k' are required to compute the maximum intercept time using Algorithm 3.3.

By combining the similarities between Algorithm 3.2 and the Algorithm described by Knuth et al [18] for generating the Stern-Brocot Tree, Algorithm 5.1 was developed to generate the adjacent elements of the Augmented, Generalized Farey Series in an iterative manner:

Algorithm for Calculating Maximum Intercept Time

The modification to Algorithm 3.3 in order to utilize Algorithm 5.1 is outlined in Algorithm 5.2.

5.3.3 Reproduction

The selection operator was stochastic universal sampling [19], which provided a fair sampling of individuals. The effects of the elite count were examined by iterating through the GA with an elite count varying from 0 to 10 (Figure 5.1). No significant effects on the rate of minimization were observed, so the elite count was set to zero.

5.3.4 Crossover

The crossover operator was a random multi-point operator, where genes from both parents were randomly swapped along the length of the individual. The effects of the crossover fraction were examined by iterating through the GA with fractions ranging from 0 to 1 and plotting the results (Figure 5.1). A crossover value of 0.8 provided the best rate of minimization. This value gave the best balance between improvement generated through crossover vs improvement generated through mutation.

input : $(\lambda_1, \lambda_2, T_1, T_2)$, where T_n is the PRI and λ_n are the duty cycles for pulse train n
output: $(\mathfrak{G}_L^*, \mathfrak{G}_R^*)$, the adjacent elements to $\alpha = T_2/T_1$ of the Augmented, Generalized Farey Series elements

```
1  proc (G*_L, G*_R) = augfarey2(λ1, λ2, T1, T2):
2  begin
3      α = T2/T1;
4      h = 0, k = 1, h' = 1, k' = 0;
5      while (λ1(k + k') + λ2(h + h')) < 1 do
6          h_mediant = h + h';
7          k_mediant = k + k';
8          if α < (h_mediant / k_mediant) then
9              h' = h_mediant;
10             k' = k_mediant
11         else
12             h = h_mediant;
13             k = k_mediant
14         end
15     end
16     G*_L = h/k, G*_R = h'/k';
17 end
```

Algorithm 5.1: An Iterative Method for Producing the Augmented, Generalized Farey Series

input : $(T_1, T_2, \lambda_1, \lambda_2)$, where T_n is the PRI and λ_n are the duty cycles for pulse train n
output: t, the maximum intercept time

```
1  proc t = intercepttime2(T_1, T_2, λ_1, λ_2)): ;
2  begin
3      α = T_2/T_1;
4      (h/k, h'/k') = augfarey2(λ_1, λ_2, T_1, T_2);
5      if α = h/k or α = h'/k' then
6          t = ∞
7      else
8          if k < k' then
9              x = (h+λ_1)/(k−λ_2)
10         else
11             x = (h'−λ_1)/(k'+λ_2)
12         end
13         if α < x or (k < k' and α = x) then
14             (p, q, P, Q) = (h, k, h', k')
15         else
16             (p, q, P, Q) = (h', k', h, k)
17         end
18         κ = ⌊(ε−|Qα−P|)/|qα−p|⌋;
19         t = T_2(Q + q − κq);
20     end
21 end
```

Algorithm 5.2: Calculating Maximum Intercept Time

The effects of elitism were also examined over the range 0 to 10 on a population of 100 (Figure 5.1). No significant impact was noticed so elitism was not used (0 elites).

5.3.5 Mutation

The mutation operator was Gaussian mutation [20]. The mutation was controlled by two variables, *Scale* and *Shrink*. *Scale* was used to generate a range for the mutated values of *Scale*(max duration - min duration), where the minimum and maximum durations were the same as those defined for the initial population (see section 5.3.1). *Shrink* controlled the variance of the mutation. The highest degree of variance was used in the first generation, which decreased as the number of generations increased. The variance at the kth generation was determined by

$$var_k = var_{k-1}\left(1 - Shrink \cdot \frac{k}{MaxGeneration}\right)$$

Several combinations of *Scale* and *Shrink* were tried, and a *Scale* value of 0.1 and a *Shrink* value of 0.75 provided the fastest rate of minimization. These values ensured the GA examined the search space within the vicinity of the current solution. This was desirable because of the highly non-linear nature of the objective function, where small variations could cause large deviations. As each generation was calculated, the decrease in variance was limited (i.e. it did not decrease to zero). This ensured that the small area available for mutation was well searched and that movement between closely space local minima was not limited.

5.3.6 Terminating Conditions

The terminating condition for the GA was the completion of 400 generations. While other valid terminating conditions were possible and were attempted, the comparison of different simulations with differing generations became a problem. A Monte-Carlo approach was deemed necessary to account for the heuristic nature of the GA, and summarizing the results correctly required simulations with an equivalent number of generations. No significant improvement of the objective function was noticeable after approximately 300 generations, but the extra 100 generations were run to allow the scheduler plenty of opportunity to search the space. The 'no significant improvement'

of the objective function could be measured in milliseconds.

5.3.7 Multiple Runs

Since the use of genetic algorithms is a heuristic technique that relies on randomness during execution, we expect the results to vary slightly between simulations. The GA scheduler for each scenario was run 1000 times in a Monte-Carlo manner to verify it produced consistent results. This number of runs was required to generate histograms that approximated a normal distribution.

5.4 Pseudo-Random Scheduler Setup

The Pseudo-Random (PR) scheduler was set up to naively enumerate a schedule with randomly generated durations. The duration values were uniformly distributed between a minimum duration value of $10t_{pulsePRI}$ using the minimum $t_{pulsePRI}$ value from all the emitters (the minimum time required for coincidence) and a maximum duration value set at 20 s, an arbitrary value that exceeded all the emitter scan rates.

In order to examine the effects of phase, 10 pulse trains were created for each emitter, each pulse train corresponding to a phase ranging from 0 to 90 percent of the emitter scan rate (in 10 percent increments).

Intercept times were then determined by comparing the random pulse train of the schedule with the periodic pulse trains of each emitter and phase. Each coincidence between the pulse trains was examined, and the first coincidence that exceeded the minimum duration required for intercept ($10t_{pulsePRI}$ for the emitter) was deemed an intercept. The maximum value from each phase was deemed the maximum intercept time. The scheduler ran for the simulation times shown in Table 5.4. Each scenario ran 60 times.

Scenario	Simulation Time
SESB	1000 s
SEMB	2500 s
MESB	1500 s
MEMB100	8800 s

Table 5.4 Maximum Simulation Times for the PR Scheduler

5.5 Results

The results from each scenario are presented as they were generated by each scheduler. A summary is then provided which allows an easy comparison of the results between schedulers.

5.5.1 Genetic Algorithm Results

A histogram of the schedule intercept time results generated by the GA scheduler was generated for each scenario, and is displayed at Figure 5.2. Each histogram shows the schedule intercept time on the x-axis, and the y-axis shows the number of schedules that have intercept times in the various x-axis ranges.

Box plots were created that summarize the schedule durations for each scenario, and are displayed in Figures 5.4 to 5.7. In each box plot, the frequency bands are displayed on the x-axis and the range of durations is displayed on the y-axis. As shown in Figure 5.3, the bar indicates the median duration, the box surrounding the bar indicates the interquartile range (the range from the 75th percentile to the 25th percentile), and the upper and lower whiskers indicate the extent of the maximum and minimum duration values.

5.5.2 Pseudo-Random Results

The simulation times for each run were picked so that the pseudo-random scheduler was able to consistently find intercepts for each phase of each emitter.

The maximum intercept time values were averaged over the multiple runs. The schedule and emitter intercept times are contained in Tables 5.5 and 5.6.

5.5.3 Summarized Results

A summary of the GA, PR, and MS results are presented in Tables 5.5 and 5.6. Table 5.5 contains the results of the schedule intercept times generated by each scheduler, and Table 5.6 contains the emitter intercept times generated by the best schedule (shortest schedule intercept time) from each scheduler.

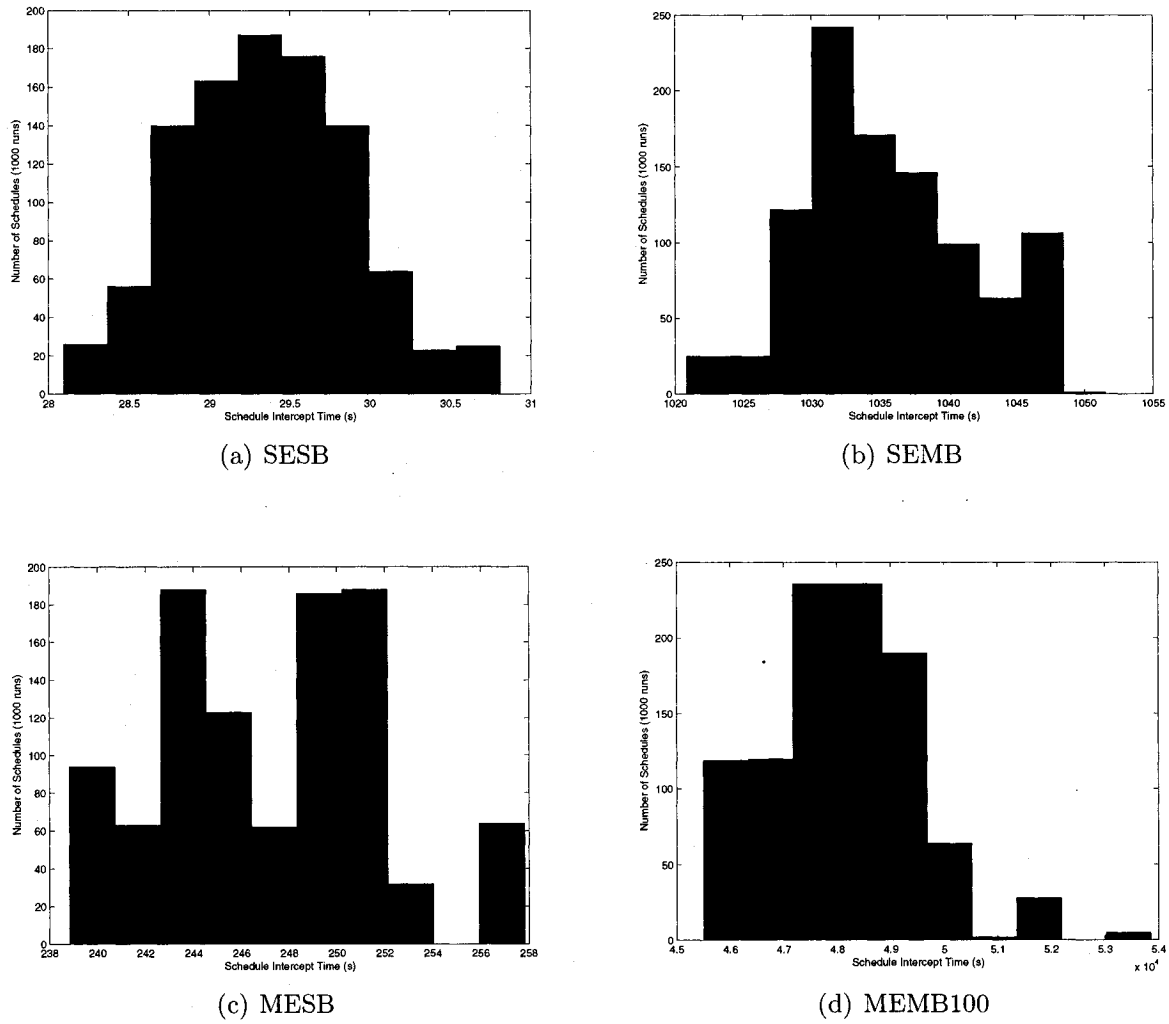

(a) SESB (b) SEMB

(c) MESB (d) MEMB100

Fig. 5.2 Histogram of Schedule Intercept Times (GA Scheduler)

5.6 Analysis

The experiment generated many results, some of which were unexpected. The genetic algorithm scheduler produced the best results when compared with the pseudo-random scheduling technique, and provided some insight into a new scheduling algorithm.

5.6.1 Expected Results

The genetic algorithm scheduler was expected to produce the best results (shortest schedule intercept time). Balancing the durations in each frequency band (and the

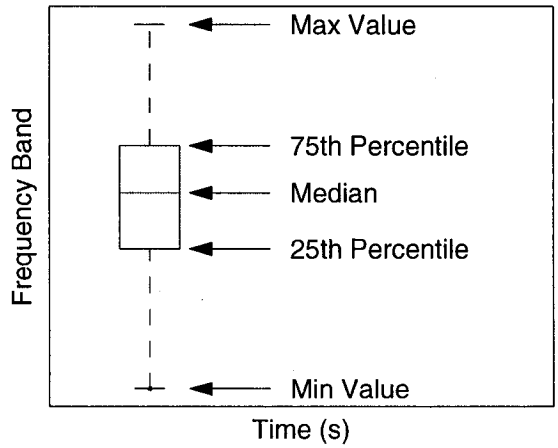

Fig. 5.3 Sample Box Plot

Scenario	Scheduler	Min Schedule Intercept Time	Max Schedule Intercept Time	Mean Schedule Intercept Time
SESB	GA	28.093 s	30.811 s	29.351 s
	PR	16.800 s	1059.2 s	316.76 s
SEMB	GA	1020.8 s	1051.5 s	1035.5 s
	PR	2897.2 s	6681.4 s	4943.6 s
MESB	GA	238.83 s	257.82 s	247.25
	PR	757.24 s	5315.6 s	2295.8 s
MEMB100	GA	45505 s	53856 s	48138 s
	PR	13489 s	94966 s	46167 s

Table 5.5 Schedule Intercept Time Statistics

impact of these on the maximum intercept time calculations) with the minimum coincidence durations and the slew time constraints fit very well with the characteristics of the GA scheduler's heuristic technique. The GA scheduler was expected to find 'good' duration values that balanced the effects of the constraints. These durations were expected to be as small as possible until the slew rate constraint bounded their values. This would effectively 'slice' time between each frequency band to produce minimized intercept times for each emitter.

The pseudo-random scheduler was not expected to generate the best results. While the random durations generated by the PR scheduler were expected to break the synchronization between the receiver and the emitters, the algorithm was not expected to pick 'good' duration values that would reduce the maximum time to intercept.

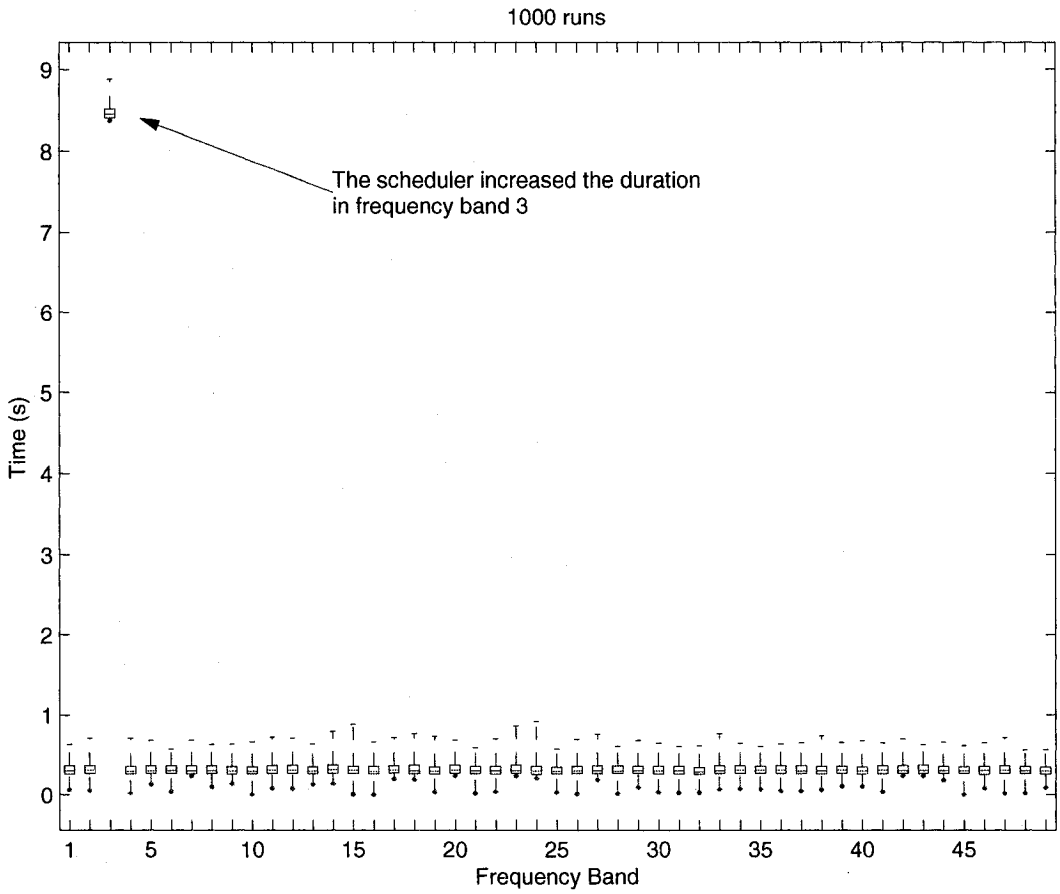

Fig. 5.4 SESB - Box Plot of Schedule Durations (GA Scheduler)

5.6.2 Comparison of Expected vs. Actual Results

As expected, the best results (lowest maximum schedule intercept time) were generated by the genetic algorithm scheduler. The pseudo-random scheduler did not consistently produce feasible schedules as it was unable to find intercepts for all emitter phases before each simulation was truncated.

5.6.3 Analysis of GA Results

The GA scheduler was consistent at finding feasible solutions, and with lower mean schedule intercept times than the PR scheduler. The histograms in Figure 5.2 show that the schedule intercept time results for each scenario were consistent between multiple runs of the scheduler.

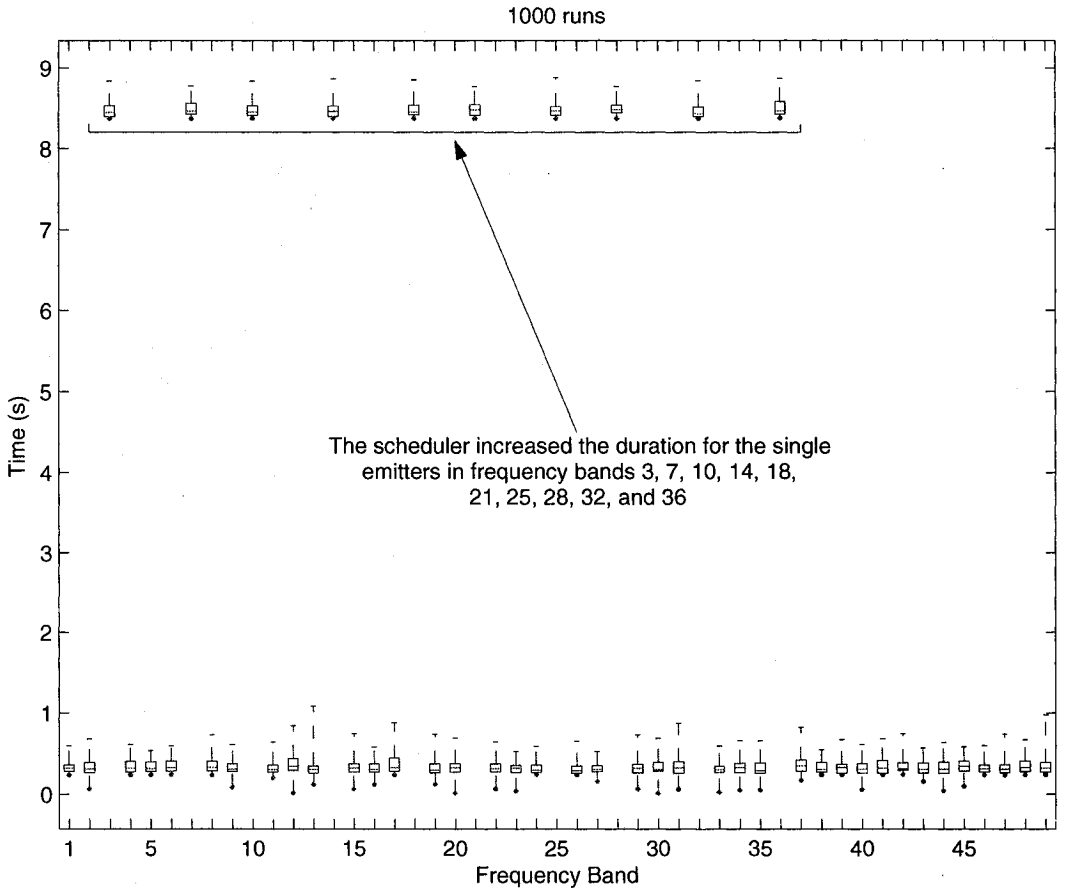

Fig. 5.5 SEMB - Box Plot of Schedule Durations (GA Scheduler)

Figures 5.4 to 5.7 show how the duration value results for each scenario were consistent between multiple runs of the scheduler. For each scenario, the scheduler picked a duration value for each frequency band that intercepted all the emitters in that band.

Surprisingly, the GA scheduler produced schedules where there was no time-slicing of the durations between frequency bands. As shown in Figure 5.8 for the MEMB100 scenario (the same observation was made for all the scenarios), the scheduler chose durations for each frequency band that were very close to the largest emitter scan rate of all the emitters in that band (Maximum-Scan rate).

With no upper limit constraining the duration in each frequency band, the durations still did not vastly exceed the emitter maximum scan rates. This can be explained by examining the effects of increased duration in any particular frequency band. As the

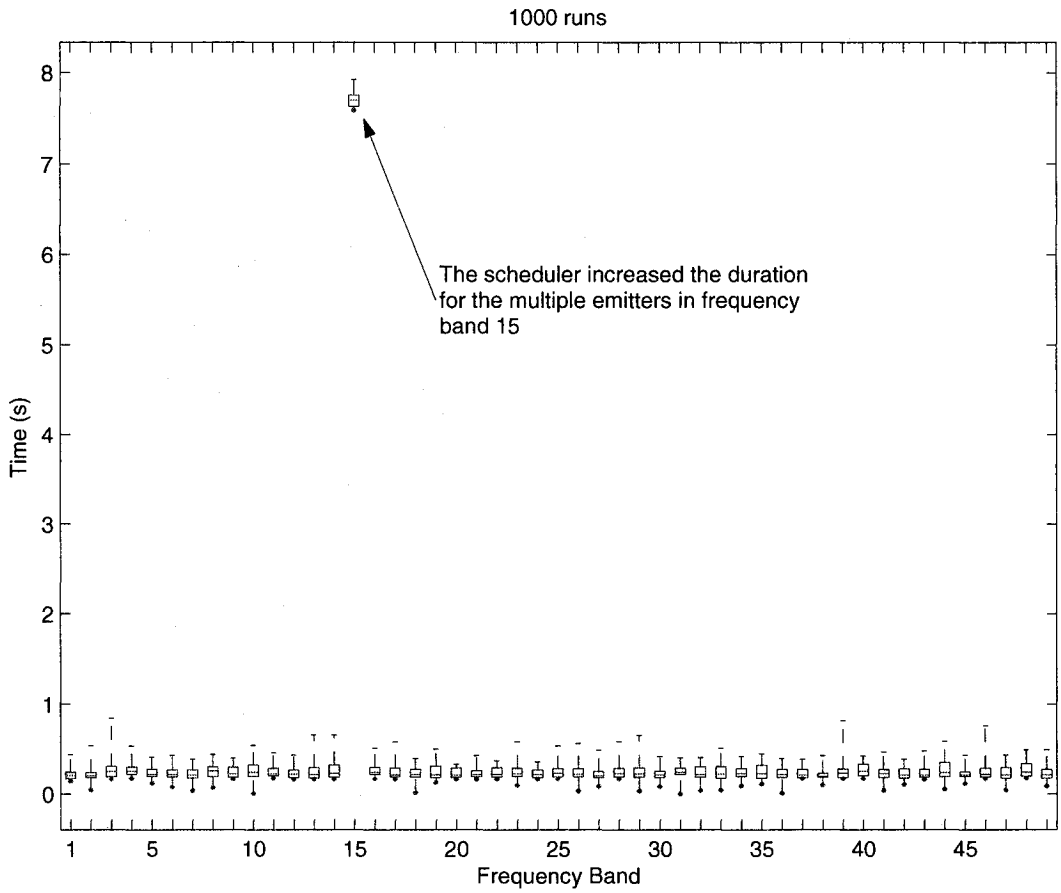

Fig. 5.6 MESB - Box Plot of Schedule Durations (GA Scheduler)

duration increased, the maximum intercept time decreased for each emitter. The longer duration caused more overlap of the pulse trains, and hence more intercepts with less number of pulses. When the duration exceeded the maximum scan rate, there was no further decrease in maximum intercept time - the emitter was intercepted on the first 'look' from the receiver. However, an increase to any duration past that point increased the maximum intercept time (by increasing the intercept times for following frequency bands), so the scheduler did not increase the duration any further. Any emitter with a scan rate lower than the emitter with the largest scan rate was always intercepted (sometimes multiple times) because of a complete overlap of the pulse trains.

The slew time and minimum duration constraints were not active in frequency bands that contained emitters. For frequency bands with no emitters, the GA scheduler tried

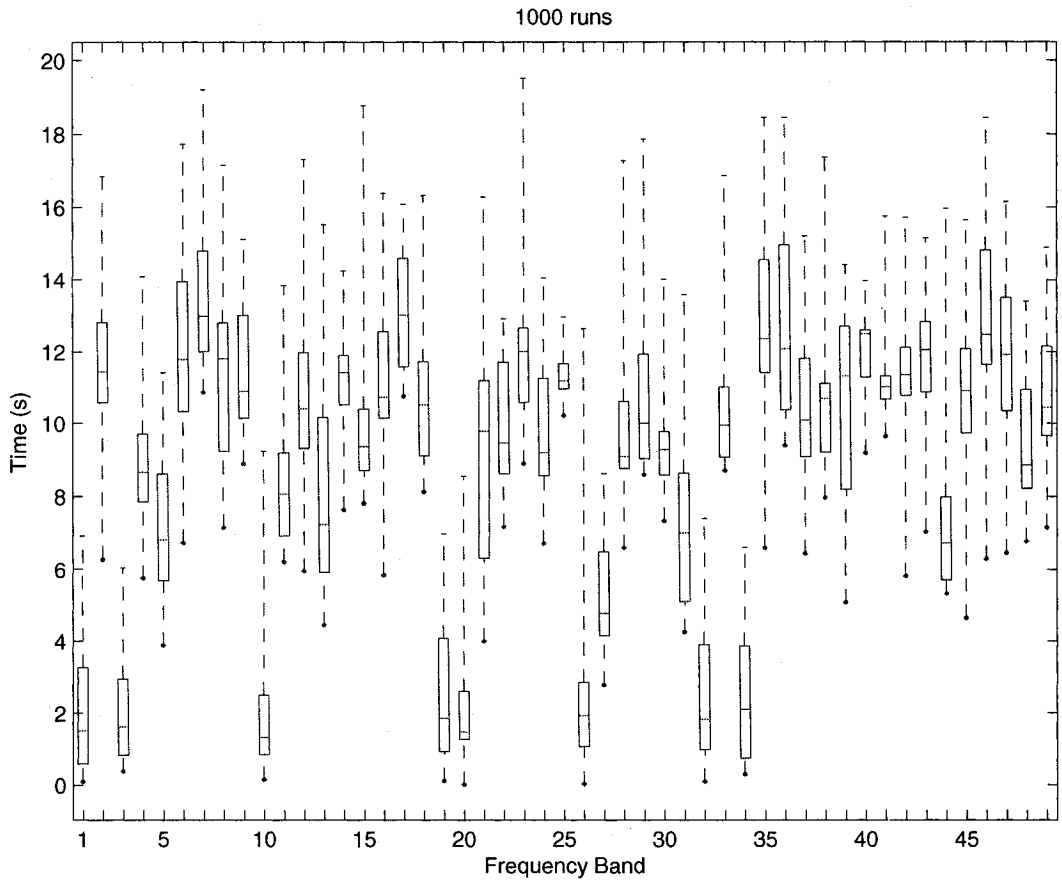

Fig. 5.7 MEMB100 - Box Plot of Schedule Durations (GA Scheduler)

to shorten the duration in that band to the minimum possible value, which was set as a constraint.

5.6.4 Maximum-Scan Scheduling

The GA scheduler consistently generated schedules where the durations appeared to stabilize at the maximum-scan (MS) values. As this became apparent, the results were incorporated into the experiment with the intent of improving the results.

The GA scheduler was initialized with an initial population that contained a MS-valued genome, and each scenario was re-run. If the genome with the MS values was a 'good' initial solution, the GA scheduler was expected to choose it for continued iterations.

Scenario	Scheduler	Min. Emitter Intercept Time	Max. Emitter Intercept Time	Mean Emitter Intercept Time
SESB	GA	28.093 s	28.093 s	28.093 s
	PR	16.800 s	1059.2 s	316.76 s
SEMB	GA	102.08 s	102.08 s	102.08 s
	PR	16.800 s	2137.8 s	494.36 s
MESB	GA	23.883 s	23.883 s	23.883 s
	PR	72.614 s	1231.0 s	229.58 s
MEMB100	GA	437.56 s	875.09 s	455.05 s
	PR	1.1077 s	3216.4 s	372.31 s

Table 5.6 Emitter Intercept Time Statistics (Best Schedule)

A naive maximum-scan scheduling technique was also created to verify what the MS values could produce. This technique was the equivalent of the receiver 'staring' at a frequency band until all the emitters in that band had been intercepted. This would guarantee that a periodically scanning emitter would always be intercepted the first time the receiver 'looked' for it.

Genetic Algorithm with Maximum-Scan Initial Values

The GA scheduler was initially set up exactly as specified in section 5.3. A single individual from the initial population was randomly selected and replaced with an individual containing the maximum-scan values for that scenario.

After this modified GA scheduler was run several times, it was observed that the objective function value would degrade (i.e. it would increase) for several generations. After these generations, the objective function value would then improve (i.e. decrease), but never to a value lower than that from the first generation.

This was explained by the fact that the best individual in the initial population was the individual with the MS values. As it was selected for reproduction and crossover, the MS value genes were combined with the randomly valued genes of other individuals. With the elite count at zero, the MS valued individual was then discarded. Only after the offspring of the MS valued individual were propagated sufficiently through the population (which took several generations) was the objective function able to improve. The MS valued individual was essentially 're-bred' after it's genes were prevalent enough in the population, and the scheduler could not find a way to improve the fitness.

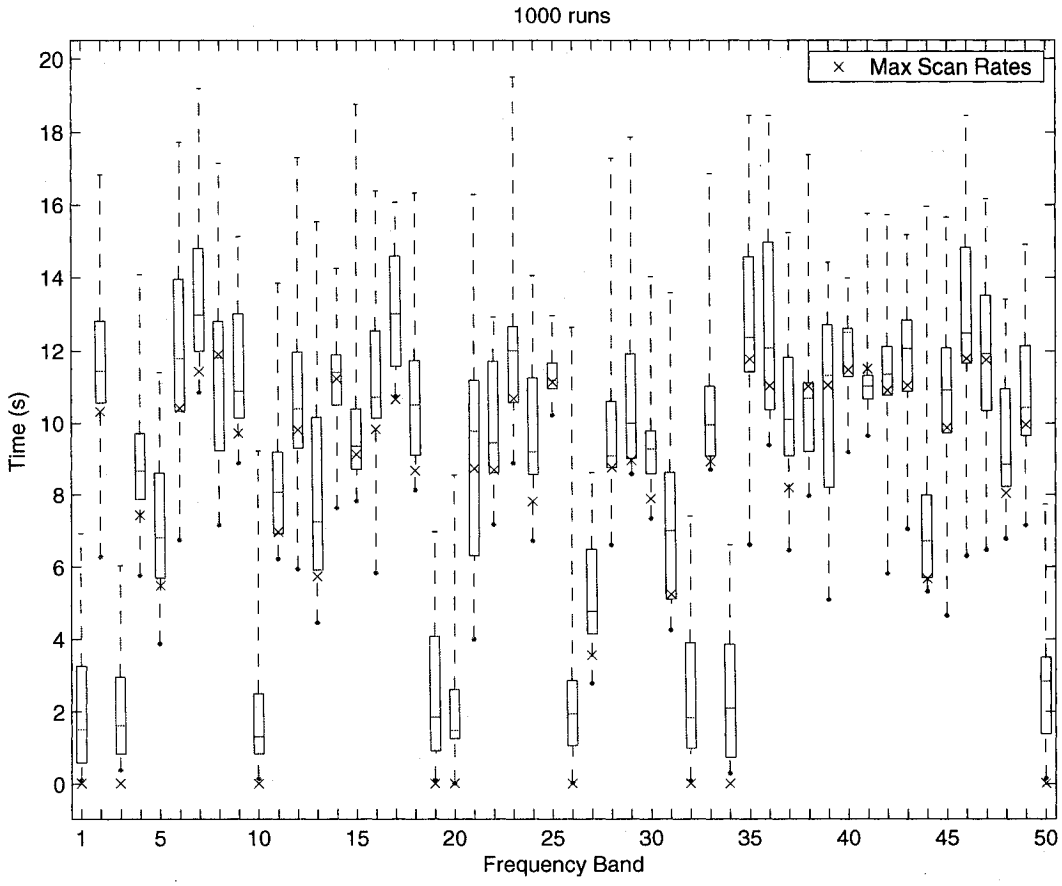

Fig. 5.8 Comparison of GA results (MEMB100) with Maximum Emitter Scans

After observing this phenomenon, the elite count was set to one and the modified GA scheduler was run again. The objective function value did not change with any number of generations, and the MS valued individual was always kept from generation to generation.

Maximum-Scan Scheduler Setup

The Maximum-Scan (MS) scheduler was set up to naively enumerate a schedule with durations generated from the emitter values. The emitters were divided into the frequency bands of the SHR, and the emitter with the longest scan rate in each band was chosen. This scan rate was used as the duration for the band. If no emitter existed in a particular frequency band, a minimum duration of $10t_{pulsePRI}$ was chosen for the

emitter with the smallest $t_{pulsePRI}$ over all the emitters.

To account for the starting phases of the receiver and emitter, the worst possible combination of phase was calculated as the larger of either the emitter phase or the receiver phase. Since the receiver phase was always longer, the maximum intercept time for each emitter used the value

$$t_{MS} = \left(\sum_{m=1}^{M} d_{m_{MS}} \right) + M(t_{tune}) \tag{5.2}$$

where M is the number of frequency bands and t_{tune} is the time required for the receiver to change frequency bands.

Scenario	Scheduler	Min Schedule Intercept Time	Max Schedule Intercept Time	Mean Schedule Intercept Time
SESB	GA (Original)	28.093 s	30.811 s	29.351 s
	GA (MS Init)	14.569 s		
	MS	14.569 s		
SEMB	GA (Original)	1020.8 s	1051.5 s	1035.5 s
	GA (MS Init)	899.545 s		
	MS	899.545 s		
MESB	GA (Original)	238.83 s	257.82 s	247.25
	GA (MS Init)	134.394 s		
	MS	134.394 s		
MEMB100	GA (Original)	45505 s	53856 s	48138 s
	GA (MS Init)	38808 s		
	MS	38808 s		

Table 5.7 Maximum Scan Schedule Intercept Time Statistics

5.6.5 Analysis of MS Results

The results for the GA scheduler initialized with the maximum-scan values, and the MS scheduler are presented in Tables 5.7 and 5.8. The modified GA scheduler was not able to improve the schedule intercept time (400 generations). The maximum scan scheduler produced equivalent results to the modified GA scheduler.

Scenario	Scheduler	Min. Emitter Intercept Time	Max. Emitter Intercept Time	Mean Emitter Intercept Time
SESB	GA (Original)	28.093 s	28.093 s	28.093 s
	GA (MS Init)	14.569 s		
	MS	14.569 s		
SEMB	GA (Original)	102.08 s	102.08 s	102.08 s
	GA (MS Init)	89.955 s		
	MS	89.955 s		
MESB	GA (Original)	23.883 s	23.883 s	23.883 s
	GA (MS Init)	13.439 s		
	MS	13.439 s		
MEMB100	GA (Original)	437.56 s	875.09 s	455.05 s
	GA (MS Init)	388.09 s		
	MS	388.09 s		

Table 5.8 Maximum Scan Emitter Intercept Time Statistics (Best Schedule)

5.6.6 Analysis of PR Results

The results of the pseudo-random scheduler have several flaws that make comparison with the other schedulers difficult. First, the PR scheduler did not enumerate all the phases of each emitter. Only 10 phases were included, and although they were evenly distributed from 0 to 90 % of the emitter scan rate, it is possible that phases exist that could not be found by the scheduler. Secondly, the simulations for the PR scheduler did not account for the receiver starting phase. The minimum schedule and emitter intercept times would be different for different receiver starting phases.

While these flaws existed, the results were still useful for comparison with the GA scheduler, and produced some unexpected values. The PR scheduler generally performed worse than the GA and GA/MS schedulers, especially for scenarios where there were few emitters. This poor performance was related to the amount of time that the PR scheduler dwelled in frequency bands where there were no emitters. This dwell time increased the intercept time for every other band. The PR minimum schedule and emitter intercept times were sometimes better than the GA scheduler because of the PR starting phase, but this was solely related to the receiver starting phase. If the emitter was in later bands (or the receiver started in a different frequency band), the intercept times would have been correspondingly longer.

As the emitter density grew, the number of bands without emitters decreased, and the performance of the PR scheduler increased. For the MEMB100 scenario, most bands contained emitters, so a dwell time in a band increased the number of intercepts, and decreased the maximum intercept time. The PR scheduler generated mean schedule and emitter intercept times for the MEMB100 scenario that were better than the GA scheduler.

In comparison with the GA results, the PR scheduler provided minimum and no guaranteed maximum values, and provided much higher maximum intercept times.

5.6.7 Sensitivity and Variability

The genetic algorithm scheduler was very sensitive to the initial population and mutation values. The best results were obtained when the durations were constrained with maximum and minimum durations. The reason for this was the highly non-linear objective function. If no maximum or minimum durations were used, the GA scheduler still obtained the same results, but required many more generations to produce them.

5.7 Summary

The use of a genetic algorithm scheduler was successful at producing a schedule for a scanning superheterodyne receiver. The GA scheduler consistently used duration values for each frequency band that were near the highest scan rate of all the emitters in each band. Using this observation, the GA scheduler was initialized to these values, and it could not obtain a better solution. A new scheduler was created that naively used the maximum scan rates to generate the duration values, and it produced the same results as the GA scheduler that was initialized with the maximum scan values, with much less computational effort.

Chapter 6

Conclusion

The combination of genetic algorithms with pulse train theory was successful at producing a schedule for an ESM receiver. The genetic algorithm scheduler consistently used duration values for each frequency band that were near the largest scan rate of all the emitters in each band. This was an unexpected result and demonstrated that the minimization of the maximum intercept time for a set of emitters can be accomplished using the maximum scan values.

A scheduling algorithm was created that utilized the maximum scan values. It generated ESM receiver schedules that were equivalent to the best schedules produced by the genetic algorithm scheduler, and produced them with much less computational effort.

The schedules that were created by both the genetic algorithm scheduler and the maximum scan scheduler produced emitter intercept times that were very long. Hundreds of seconds to intercept an emitter is typically an intolerably long time in ESM applications. However, the schedules have generated a maximum time to intercept; the mean time to intercept will depend on the phases of the emitter and receiver pulse trains, and may be much less.

The creation of ESM receiver schedules is a difficult and important task for those involved in the interception of radar signals. Radar emitters are growing in capability and diversity, and are a continuous threat on the modern battlefield. ESM systems are important contributors to situational awareness, and determining methods to utilize the full potential of these resources will continue to be a sound investment.

6.1 Suggestions for Future Research

The following suggestions are made for future research:

- Investigate the effects of time-slicing between frequency bands. The originally expected result of a time-sliced schedule is still an area open for study. If constraints are introduced on the maximum durations that can be used in each frequency band, what are the effects of these on the maximum intercept time? The relationship between schedules that optimize for maximum bandwidth scanning per unit time needs to be quantified against schedules that optimize for maximum intercept time.

- The effects of an individual emitter on a complete schedule are not well understood. If an emitter is removed or added from the emitter list, what impact does that have on the maximum intercept time? Can this impact be quantified?

- Investigate the use of an optimization technique such as genetic algorithms to generate schedules that minimize the mean time to intercept for a set of scanning emitters. The maximum intercept time is very useful, but it is not the only performance measure available, and would be well complemented by the mean intercept time.

- Investigate the modification of the receiver schedule in an adaptive manner during receiver operation. If a periodic emitter is intercepted while a receiver is scanning, the next (and subsequent) transmissions can easily be calculated. Is it possible to reduce the duration of the receiver in that emitters frequency band? If it is possible, how much should it be changed? This will change the receiver schedule period, so what would be the impact on the maximum intercept time?

Appendix A

Emitter Data

Table A.1 SESB Emitter Data

No.	F	PRI	T_{scan}	λ_{scan}
1	2.00 GHz	2.386330 ms	8.40 s	0.0030429

Table A.2 SEMB Emitter Data

No.	F	PRI	T_{scan}	λ_{scan}
1	2.10 GHz	2.386330 ms	8.40 s	0.0030429
2	3.90 GHz	2.386330 ms	8.40 s	0.0030429
3	5.70 GHz	2.386330 ms	8.40 s	0.0030429
4	7.50 GHz	2.386330 ms	8.40 s	0.0030429
5	9.30 GHz	2.386330 ms	8.40 s	0.0030429
6	11.10 GHz	2.386330 ms	8.40 s	0.0030429
7	12.90 GHz	2.386330 ms	8.40 s	0.0030429
8	14.70 GHz	2.386330 ms	8.40 s	0.0030429
9	16.50 GHz	2.386330 ms	8.40 s	0.0030429
10	18.30 GHz	2.386330 ms	8.40 s	0.0030429

Table A.3 MESB Emitter Data

No.	F	PRI	T_{scan}	λ_{scan}
1	8.00 GHz	5.418742 ms	6.75 s	0.0881341
2	8.00 GHz	5.514937 ms	3.99 s	0.0259806
3	8.00 GHz	4.496685 ms	2.50 s	0.0181639
4	8.00 GHz	2.236380 ms	4.29 s	0.0664828
5	8.00 GHz	3.370742 ms	1.71 s	0.0988452
6	8.00 GHz	3.178684 ms	6.67 s	0.0340612
7	8.00 GHz	2.348989 ms	7.38 s	0.0762761
8	8.00 GHz	4.090211 ms	3.30 s	0.0386020
9	8.00 GHz	4.259552 ms	6.07 s	0.0572150
10	8.00 GHz	1.648567 ms	7.63 s	0.0059766

Table A.4: MEMB100 Emitter Data

No.	F	PRI	T_{scan}	λ_{scan}
1	13.16 GHz	1.797600 ms	9.71 s	0.0273970
2	12.96 GHz	3.126869 ms	8.60 s	0.0259943
3	13.86 GHz	5.156397 ms	3.51 s	0.0867866
4	5.22 GHz	1.780437 ms	8.58 s	0.0789118
5	24.80 GHz	2.838795 ms	9.94 s	0.0620121
6	23.82 GHz	2.044534 ms	11.73 s	0.0296313
7	7.51 GHz	3.120441 ms	4.36 s	0.0622921
8	19.58 GHz	4.510228 ms	6.26 s	0.0597872
9	7.08 GHz	3.078491 ms	5.71 s	0.0718073
10	16.15 GHz	1.872294 ms	5.22 s	0.0932047
11	9.08 GHz	4.653633 ms	10.63 s	0.0048320
12	15.67 GHz	4.377531 ms	5.08 s	0.0946003
13	18.38 GHz	2.960216 ms	9.32 s	0.0270812
14	5.88 GHz	2.589813 ms	6.93 s	0.0497300
15	7.65 GHz	2.335764 ms	11.21 s	0.0874644
16	5.77 GHz	5.034410 ms	6.43 s	0.0395221
17	1.33 GHz	1.691551 ms	2.22 s	0.0875999

Continued on next page

No.	F	PRI	T_{scan}	λ_{scan}
18	16.80 GHz	4.661460 ms	7.52 s	0.0935375
19	20.89 GHz	2.846186 ms	5.75 s	0.0558757
20	14.44 GHz	2.099700 ms	8.75 s	0.0592432
21	5.08 GHz	5.481098 ms	5.13 s	0.0408765
22	11.96 GHz	5.504966 ms	8.94 s	0.0742614
23	19.25 GHz	4.425113 ms	3.98 s	0.0614646
24	2.27 GHz	3.771203 ms	6.18 s	0.0970295
25	21.15 GHz	4.747527 ms	11.46 s	0.0761346
26	5.20 GHz	2.982082 ms	9.69 s	0.0175082
27	22.12 GHz	5.143786 ms	5.73 s	0.0552682
28	22.44 GHz	3.550831 ms	5.64 s	0.0613446
29	20.48 GHz	3.988689 ms	9.57 s	0.0695291
30	3.90 GHz	4.307371 ms	10.57 s	0.0789917
31	4.67 GHz	3.283458 ms	5.42 s	0.0970469
32	24.64 GHz	3.534349 ms	6.91 s	0.0359500
33	14.39 GHz	1.639482 ms	4.82 s	0.0890089
34	12.84 GHz	4.110638 ms	11.09 s	0.0837311
35	6.17 GHz	4.339509 ms	6.43 s	0.0578648
36	20.98 GHz	1.952186 ms	8.61 s	0.0702946
37	15.18 GHz	2.598196 ms	8.40 s	0.0771879
38	19.34 GHz	1.819293 ms	11.00 s	0.0995365
39	24.48 GHz	2.813104 ms	8.01 s	0.0130569
40	23.27 GHz	2.172387 ms	1.77 s	0.0148782
41	2.44 GHz	2.483675 ms	7.41 s	0.0558603
42	7.87 GHz	5.062557 ms	7.64 s	0.0176172
43	22.41 GHz	1.456599 ms	5.46 s	0.0381740
44	13.24 GHz	2.716863 ms	4.85 s	0.0871736
45	9.31 GHz	3.301557 ms	7.33 s	0.0458288
46	4.19 GHz	2.585145 ms	5.95 s	0.0972846
47	24.16 GHz	3.358922 ms	2.52 s	0.0706584

Continued on next page

No.	F	PRI	T_{scan}	λ_{scan}
48	14.11 GHz	3.019498 ms	1.93 s	0.0885051
49	9.47 GHz	4.738354 ms	2.03 s	0.0494276
50	20.40 GHz	4.042357 ms	6.80 s	0.0072973
51	7.64 GHz	1.402148 ms	3.44 s	0.0839391
52	1.50 GHz	3.667153 ms	10.29 s	0.0058277
53	9.07 GHz	3.926444 ms	10.62 s	0.0237746
54	3.25 GHz	3.975251 ms	5.45 s	0.0957959
55	21.53 GHz	3.157808 ms	10.87 s	0.0854505
56	16.91 GHz	4.300434 ms	8.89 s	0.0396295
57	4.18 GHz	2.315539 ms	2.94 s	0.0276751
58	16.79 GHz	2.629983 ms	2.53 s	0.0763788
59	9.51 GHz	5.468325 ms	8.63 s	0.0636587
60	11.07 GHz	2.996473 ms	8.71 s	0.0261936
61	20.64 GHz	1.527296 ms	5.07 s	0.0125489
62	15.21 GHz	4.208155 ms	8.93 s	0.0648965
63	17.85 GHz	4.564396 ms	11.73 s	0.0114942
64	21.26 GHz	3.538085 ms	1.10 s	0.0383053
65	19.64 GHz	5.593650 ms	3.09 s	0.0558030
66	6.49 GHz	1.718818 ms	9.80 s	0.0550373
67	8.20 GHz	4.499719 ms	9.08 s	0.0697027
68	14.04 GHz	2.975929 ms	2.26 s	0.0936222
69	4.26 GHz	3.223620 ms	11.87 s	0.0690171
70	15.52 GHz	2.659275 ms	7.86 s	0.0753095
71	19.02 GHz	3.454866 ms	8.16 s	0.0157066
72	11.09 GHz	2.045102 ms	2.84 s	0.0737503
73	14.98 GHz	4.039454 ms	1.16 s	0.0904640
74	19.64 GHz	4.813706 ms	1.20 s	0.0708769
75	23.80 GHz	1.592706 ms	5.16 s	0.0419684
76	8.23 GHz	5.063407 ms	4.68 s	0.0516153
77	12.93 GHz	1.763654 ms	1.29 s	0.0137612

Continued on next page

No.	F	PRI	T_{scan}	λ_{scan}
78	11.68 GHz	2.540545 ms	3.19 s	0.0708869
79	4.13 GHz	4.517547 ms	11.39 s	0.0501202
80	19.16 GHz	1.799629 ms	5.79 s	0.0501169
81	23.92 GHz	3.417226 ms	6.19 s	0.0124753
82	3.44 GHz	2.187102 ms	10.39 s	0.0183930
83	3.56 GHz	5.085828 ms	3.78 s	0.0934025
84	14.68 GHz	2.499293 ms	5.27 s	0.0823717
85	20.09 GHz	4.072721 ms	11.01 s	0.0047722
86	23.37 GHz	4.759986 ms	11.75 s	0.0088655
87	8.75 GHz	1.705648 ms	1.17 s	0.0149028
88	12.55 GHz	4.476332 ms	7.76 s	0.0902846
89	8.36 GHz	1.503575 ms	9.81 s	0.0018892
90	17.03 GHz	5.049121 ms	2.21 s	0.0274648
91	20.52 GHz	2.084643 ms	11.46 s	0.0483679
92	11.65 GHz	5.118360 ms	8.65 s	0.0447024
93	22.85 GHz	2.210459 ms	9.85 s	0.0022543
94	21.79 GHz	2.347294 ms	11.02 s	0.0543277
95	13.22 GHz	3.405658 ms	9.33 s	0.0081385
96	11.75 GHz	3.737724 ms	10.65 s	0.0313668
97	8.24 GHz	1.909030 ms	4.40 s	0.0044015
98	18.71 GHz	2.884612 ms	11.01 s	0.0707788
99	18.24 GHz	2.353691 ms	3.88 s	0.0464478
100	24.28 GHz	1.757232 ms	5.44 s	0.0131914

References

[1] S. Lekic, *NATO onslaught against Yugoslavia offers lessons for attack on Iraq.* Associated Press, November 2002.

[2] *NATO Manual MC 64/7 (Electronic Warfare in NATO).* North Atlantic Treaty Organisation, 1995.

[3] M. I. Skolnik, *Introduction to Radar Systems.* McGraw-Hill, 2nd ed., 1980.

[4] R. G. Wiley, *Electronic Intelligence: The Interception of Radar Signals.* Artech House Radar Library, Artech House, 1985.

[5] D. D. Vaccaro, *Electronic Warfare Receiving Systems.* Artech House, 1993.

[6] E. W. Weisstein, *CRC Concise Encyclopedia of Mathematics.* Chapman and Hall/CRC, December 2002.

[7] O. Ore, *Number Theory and Its History.* McGraw-Hill, 1st ed., 1948.

[8] K. Miller and R. Schwarz, "On the interference of pulse trains," *Journal of Applied Physics*, vol. 24, pp. 1032–1036, August 1953.

[9] I. V. L. Clarkson, *Approximation of Linear Forms by Lattice Points with Applications to Signal Processing.* PhD thesis, The Australian National University, Canberra, 1997.

[10] I. V. L. Clarkson, J. Perkins, and I. M. Mareels, "Number theoretic solutions to intercept time problems," *IEEE Transactions on Information Theory*, vol. 42, pp. 959–971, May 1996.

[11] I. V. L. Clarkson, "The arithmetic of receiver scheduling for electronic support," IEEE Aerospace Conference, IEEE, 2003.

[12] P. I. Richards, "Probability of coincidence for two periodically recurring events," *The Annals of Mathematical Statistics*, vol. 19, pp. 16–29, March 1948.

[13] H. D. Friedman, "Coincidence of pulse trains," *Journal of Applied Physics*, vol. 25, pp. 1001–1005, August 1954.

[14] S. W. Kelly, G. P. Noone, and J. E. Perkins, "Synchronization effects on probability of pulse train interception," *IEEE Transactions on Aerospace and Electronic Systems*, vol. 32, pp. 213–220, January 1996.

[15] W. L. Winston and M. Venkataramanan, *Introduction to Mathematical Programming.* Thomson Brooks/Cole, 4th ed., 2003.

[16] D. E. Goldberg, *Genetic Algorithms in Search, Optimization, and Machine Learning.* Addison-Wesley, 1989.

[17] D. E. Goldberg, *The Design of Innovation: Lessons from and for Competent Genetic Algorithms.* Kluwer Academic Publishers, 2002.

[18] R. L. Graham, D. E. Knuth, and O. Patashnik, *Concrete Mathematics : A Foundation for Computer Science.* Addison-Wesley, 2nd edition ed., 1994.

[19] J. Baker, "Reducing bias and inefficiency in the selection algorithm," *Proceedings of the Second International Conference on Genetic Algorithms and their Application*, pp. 14–21, 1987.

[20] *Matlab Genetic Algorithm and Direct Search Toolbox User's Guide Version 1.0.* The MathWorks, Inc., 2004.